

000  
001 

# TWICE SEQUENTIAL MONTE CARLO TREE SEARCH

  
002  
003004 **Anonymous authors**

005 Paper under double-blind review

006  
007 

## ABSTRACT

  
008009  
010 Model-based reinforcement learning (RL) methods that leverage search are respon-  
011 sible for many milestone breakthroughs in RL. Sequential Monte Carlo (SMC)  
012 recently emerged as an alternative to the Monte Carlo Tree Search (MCTS) algo-  
013 rithm which drove these breakthroughs. SMC is easier to parallelize and more  
014 suitable to GPU acceleration. However, it also suffers from large variance and  
015 path degeneracy which prevent it from scaling well with increased search depth,  
016 i.e., increased sequential compute. To address these problems, we introduce Twice  
017 Sequential Monte Carlo Tree Search (TSMCTS). Across discrete and continuous  
018 environments TSMCTS outperforms the SMC baseline as well as a popular modern  
019 version of MCTS. Through variance reduction and mitigation of path degeneracy,  
020 TSMCTS scales favorably with sequential compute while retaining the properties  
021 that make SMC natural to parallelize.  
022023 

## 1 INTRODUCTION

  
024025 The objective of Reinforcement Learning (RL) is to approximate optimal policies for decision  
026 problems formulated as interactive environments. For this purpose, model-based RL algorithms that  
027 use *search* (also called planning) with a model of the environment’s dynamics for policy optimization  
028 have been tremendously successful. Examples include games (Silver et al., 2016), robotics (Hubert  
029 et al., 2021) and algorithm discovery (Fawzi et al., 2022; Mankowitz et al., 2023). These milestone  
030 approaches are all based in the Alpha/MuZero (A/MZ, Silver et al., 2018; Schrittwieser et al., 2020)  
031 algorithm family and are driven by Monte Carlo Tree Search (MCTS, see Świechowski et al., 2023).032 Like many search algorithms, the main bottleneck of MCTS is intensive compute and therefore  
033 runtime cost. Due to the sequential nature of MCTS (Liu et al., 2020; Macfarlane et al., 2024), it is  
034 challenging to address its runtime cost through parallelization and GPU acceleration (for example,  
035 with JAX, Bradbury et al., 2018) which are staples of other modern deep RL approaches. In addition,  
036 MCTS requires maintaining the entire search tree in memory. Modern GPU-acceleration approaches  
037 such as JAX require static shapes for best performance which forces memory usage to scale with the  
038 tree size and makes space complexity another possible bottleneck for GPU scalability.039 To address this, alternative search algorithms have emerged (Piché et al., 2019). These algorithms  
040 use Sequential Monte Carlo (SMC, see Chopin & Papaspiliopoulos, 2020) for policy optimization in  
041 the Control as Inference (CAI, see Levine, 2018) probabilistic inference framework for RL. SMC is  
042 used to approximate a distribution over trajectories generated by an improved policy at the root using  
043  $N$  particles in parallel. The parallel nature and lower memory cost, which scales linearly with  $N$ ,  
044 make SMC well suited for parallelization and GPU acceleration, as demonstrated by Macfarlane et al.  
045 (2024), which has also shown that SMC is competitive with MCTS for policy improvement.046 SMC however suffers from two major problems: sharply increasing variance with search depth  
047 and path degeneracy (Chopin & Papaspiliopoulos, 2020). The variance increase stems from the  
048 exponential growth in the number of possible trajectories  $s_{1:T}$  in the search depth  $T$ . Path degeneracy  
049 is a phenomenon where due to resampling eventually all particles become associated with the same  
050 state-action at the root of the search tree. This renders any additional search completely obsolete and  
051 collapses the root policy into a delta distribution causing target degeneracy (de Vries et al., 2025).  
052 These problems can cause the performance of SMC to *deteriorate* rather than *scale* with sequential  
053 compute (search depth). In contrast, MCTS scales well with sequential compute and does not suffer  
from path degeneracy.

To address these limitations of SMC we design a novel search algorithm which we call Twice Sequential Monte Carlo Tree Search (TSMCTS). We begin with a reformulation of SMC for RL which generalizes beyond the framework of CAI, simplifying the analysis and surfacing connections to MCTS. To mitigate policy target variance and degeneracy we switch the perspective of the search from estimating trajectories to estimating the value of an improved policy at the root. This facilitates incorporating the backpropagation mechanism of MCTS for value aggregation at the root. We call this intermediate algorithm SMC Tree Search (SMCTS). Building on SMCTS, TSMCTS utilizes Sequential Halving (Karnin et al., 2013) for better search resource allocation at the root. The resulting algorithm sequentially calls SMCTS at the root on a halving number of actions with doubling number of particles, in parallel (thus, twice sequential). This addresses the remaining effects of path degeneracy at the root while acting as an additional variance reduction mechanism.

We evaluate TSMCTS on a range of continuous and discrete environments, where it significantly outperforms the SMC baseline as well as a popular modern version of MCTS (GumbelMCTS, Danihelka et al., 2022). TSMCTS scales well with additional sequential compute, unlike the SMC baseline which deteriorates, while maintaining the same space and runtime complexity properties that make SMC well suited for parallelization. In ablations, we verify empirically that TSMCTS demonstrates significantly reduced estimator variance and mitigates path degeneracy.

## 2 BACKGROUND

In RL, the environment is represented by a Markov Decision Process (MDP, Bellman, 1957)  $\mathcal{M} = \langle \mathcal{S}, \mathcal{A}, \rho, R, P, \gamma \rangle$ .  $\mathcal{S}$  is a set of states,  $\mathcal{A}$  a set of actions,  $\rho$  an initial state distribution,  $R : \mathcal{S} \times \mathcal{A} \rightarrow \mathbb{R}$  a bounded possibly stochastic reward function, and  $P$  is a transition distribution such that  $P(s'|s, a)$  specifies the probability of transitioning from state  $s$  to state  $s'$  with action  $a$ . The policy of the agent  $\pi \in \Pi$  is defined as a distribution over actions  $a \sim \pi(s)$  and its optimality is defined with respect to the objective  $J_\pi$ , the maximization of the *expected discounted return* (also called value  $V^\pi$ ):

$$J_\pi = \mathbb{E}[V^\pi(s_0) | s_0 \sim \rho] = \mathbb{E}\left[\sum_{t=0}^{H-1} \gamma^t R(s_t, a_t) \middle| s_0 \sim \rho, s_{t+1} \sim P(s_t, a_t), a_t \sim \pi(s_t)\right]. \quad (1)$$

The discount factor  $0 < \gamma < 1$  is used in infinite-horizon MDPs, i.e.  $H = \infty$ , to guarantee that the values remain bounded. A state-action *Q-value function* is defined as follows:  $Q^\pi(s, a) = \mathbb{E}[R(s, a) + \gamma V^\pi(s') | s' \sim P(s, a)]$ . We denote the value of the optimal policy  $\pi^*$  with  $V^*(s) = \max_\pi V^\pi(s), \forall s \in \mathcal{S}$ . In model-based RL (MBRL) the agent uses a model of the dynamics of the environment ( $P, R$ ) to optimize its policy, often using search algorithms such as MCTS or SMC.

**Policy improvement** is used to motivate the convergence of approximate policy iteration algorithms to the optimal policy (see Danihelka et al., 2022; Oren et al., 2025b). We will prove that our formulation of SMC for RL approximates policy improvement and can be used in a similar manner to MCTS. We define policy improvement operators  $\mathcal{I} : \Pi \times \mathcal{Q} \rightarrow \Pi$  as any operator such that  $\forall s \in \mathcal{S} : V^{\mathcal{I}(\pi, Q^\pi)}(s) \geq V^\pi(s)$  and  $\exists s \in \mathcal{S} : V^{\mathcal{I}(\pi, Q^\pi)}(s) > V^\pi(s)$ , unless  $\pi$  is already an optimal policy. We define  $\mathcal{Q}$  generally as the set of all bounded functions on the state-action space  $q \in \mathcal{Q} : \mathcal{S} \times \mathcal{A} \rightarrow \mathbb{R}$ , to indicate that policy improvement operators are defined for approximate  $q \approx Q^\pi$  and exact  $Q^\pi$ .

**Greedification** The *policy improvement theorem* (Sutton & Barto, 2018) proves that *greedification* (Chan et al., 2022; Oren et al., 2025b) produces policy improvement when applied with respect to a policy  $\pi$  and its value  $Q^\pi$ . Greedification operators  $\mathcal{I}$  are operators over the same space, such that the policy  $\mathcal{I}(\pi, q)(a|s)q(s, a)$  is *greedier* than  $\pi$  with respect to  $q$ , defined as the follows:

$$\forall s \in \mathcal{S} : \sum_{a \in \mathcal{A}} \mathcal{I}(\pi, q)(a|s)q(s, a) \geq \sum_{a \in \mathcal{A}} \pi(a|s)q(s, a), \quad (2)$$

$$\exists s \in \mathcal{S} : \sum_{a \in \mathcal{A}} \mathcal{I}(\pi, q)(a|s)q(s, a) > \sum_{a \in \mathcal{A}} \pi(a|s)q(s, a), \quad (3)$$

unless  $\pi$  is already a greedy ( $\arg \max$ ) policy with respect to  $q$ . We define *strict* greedification operators  $\mathcal{I}$  as operators that satisfy a strict  $>$  inequality 2, unless  $\pi$  is already a greedy policy at  $s$ . A

108 popular strict greedification operator is that of *regularized policy improvement* (Grill et al., 2020):  
 109

$$110 \quad \mathcal{I}_{GMZ}(\pi, q)(a|s) = \frac{\exp(\beta q(s, a) + \log \pi(a|s))}{\sum_{a' \in \mathcal{A}} \exp(\beta q(s, a') + \log \pi(a'|s))} \propto \textcolor{green}{\pi}(a|s) \exp(\beta q(s, a)) \quad (4)$$

112 which trades off with an inverse-temperature parameter  $\beta$  between *greedification* (maximizing  
 113  $\sum_{a \in \mathcal{A}} \pi(a|s) q(s, a)$  with respect to  $\pi$ ) and regularization with respect to the prior policy  $\textcolor{green}{\pi}$ . We will  
 114 use greedification operators to drive the policy improvement produced by SMC and TSMCTS.  
 115

116 **Monte Carlo Tree Search** (MCTS) is used in RL to select actions in the environment and to produce  
 117 targets for training in the form of policy improvement and value bootstraps. MCTS uses a model  
 118 of the environment (either exact, as in AlphaZero (AZ), or learned, latent and/or approximate, as in  
 119 MuZero (MZ)) to construct a search tree where each node is associated with a state  $s \in \mathcal{S}$ . The root  
 120 is set to the current state of the environment  $s_0 := s$ . For convenience, we will use the subscript  $s_t$   
 121 to denote states in the planner (here MCTS and later SMC), and will clarify when not clear from  
 122 context whether it refers to states in the environment or the planner. Each node  $s_t$  maintains: (i) a  
 123 prior-policy  $\pi_\theta(s_t)$ . (ii) The mean reward  $r(s_t, a)$  for each visited action  $a$ . (iii) An estimate of the  
 124 value  $V_M(s_t)$  which is computed as the average of all  $M$  returns passed through this node.  
 125

126 MCTS repeats a three-step process: *search*, *expansion* and *backpropagation*. The tree is traversed  
 127 following a *search policy*  $\pi'$  until a non-expanded node  $s_t$  is reached. Inspired by the work of Grill  
 128 et al. (2020), modern algorithms such as GumbelMuZero (GMZ, Danihelka et al., 2022) use  $\pi' =$   
 129  $\mathcal{I}_{GMZ}(\pi_\theta, Q_M)$  (Equation 4) with a  $\beta$  parameter that increases with  $M$ , the number of visitations to  
 130 the node. Once a non-expanded node  $s_t$  has been reached, the node is *expanded* by sampling an action  
 131  $a_t$  from the prior policy  $\pi_\theta$ , expanding the transition  $r_t = \mathbb{E}[R(s_t, a_t)]$ ,  $s_{t+1} \sim P(s_{t+1}|s_t, a_t)$  (which  
 132 is traditionally deterministic) and evaluating  $Q^{\pi_\theta}(s_t, a_t) \approx r_t + \gamma V^{\pi_\theta}(s_{t+1})$ .  $V^{\pi_\theta}(s_{t+1})$  is usually  
 133 approximated with a value DNN  $v_\phi \approx V^{\pi_\theta}$ . The new evaluation is then *backpropagated* up the  
 134 search tree, through all nodes along the trajectory  $\tau_t = s_0, a_0, \dots, s_t, a_t, s_{t+1}$ , updating the running  
 135 average of the value estimates:  $V_{M+1} = \frac{1}{M+1} \sum_{i=1}^{M+1} \nu_i$ , where  $\nu_i = \sum_{j=0}^t \gamma^j r_j^i + \gamma^{t+1} v_\phi(s_{t+1}^i)$ .  
 This process is repeated  $B$  times, the search budget of the algorithm.  
 136

137 When MCTS terminates, an action is selected at the root using an improved policy  $\pi_{improved}$ . To drive  
 138 an approximate policy iteration loop, Danihelka et al. (2022) use  $\pi_{improved} := \mathcal{I}_{GMZ}(\pi_\theta, Q_M)(s_0)$ ,  
 139 where  $Q_M(s_0, a) = r(s_0, a) + \gamma \mathbb{E}_{P(s_1|s_0, a)}[V_M(s_1)]$ .  $\pi_{improved}(s_0)$  is used to train the prior policy  
 140  $\pi_\theta$  using a cross-entropy loss. The value at the root  $V_M(s_0)$  is used to produce bootstraps for  
 TD-targets (Schriftwieser et al., 2020) or value targets directly (Oren et al., 2025a).  
 141

142 **Sequential Halving with MCTS** Due to the compute budget  $B$  being known in advance in many  
 143 cases in practice, in GumbelAlpha/MuZero (GA/MZ, Danihelka et al., 2022), the authors propose to  
 144 separate MCTS to two processes: a *simple-regret* minimization at the root  $s_0$  through the Sequential-  
 145 Halving (SH, Karnin et al., 2013) algorithm. At all other nodes the original MCTS process is  
 146 used. SH begins with a set  $|A_1| = m_1$  of actions to search and a total search budget  $B$ . SH then  
 147 divides the search budget equally across  $i = 1, \dots, \log_2 m_1$  iterations. The per-iteration budget  
 148 itself is divided equally across the actions searched this iteration  $A_i$ . As its name suggests, SH  
 149 halves the number of actions that are searched each iteration by taking the top half according to a  
 150 certain statistic,  $\arg \max \mathcal{I}_{GMZ}(\pi_\theta, Q_{\textcolor{green}{M}})(s_0)$  in the case of GA/MZ. As a result, at each iteration  
 151 the search budget for the remaining actions doubles. After the final iteration the algorithm returns  
 152 the improved policy  $\pi_{improved}(s_0) = \mathcal{I}_{GMZ}(\pi_\theta, Q_{\log_2 m_1})(s_0)$ , and the value of the root state  
 153  $V_{search}(s_0) = \sum_{a \in A_1} \pi_{improved}(a|s_0) Q_{\log_2 m_1}(s_0, a)$ .  
 154

155 **Sequential Monte Carlo** (SMC) methods approximate a sequence of *target distributions*  $p_t(x_{0:t})$   
 156 using *proposal distributions*  $u_t(x_t | x_{0:t-1})$ . At each time step  $t \in \{0, \dots, T\}$ ,  $N$  particles  $x_t^n$   
 157 with weights  $w_t^n$  are updated via *mutation, correction, and selection* (Chopin, 2004). *Mutation*:  
 158 each trajectory  $x_{0:t-1}^n$  is extended by sampling  $x_t^n \sim u_t(x_t | x_{0:t-1}^n)$ . *Correction*: The weights are  
 159 updated to account for the target distribution, such that the set of weighted particles  $\{x_t^n, w_t^n\}_{n=1}^N$   
 approximates expectations under the target:  
 160

$$161 \quad w_t^n = w_{t-1}^n \cdot \frac{p_t(x_t^n | x_{0:t-1}^n)}{u_t(x_t^n | x_{0:t-1}^n)}, \quad \frac{\sum_{n=1}^N w_t^n f(x_t^n)}{\sum_{n=1}^N w_t^n} \approx \mathbb{E}_{p_t}[f(x_t)], \quad (5)$$

162 where  $f(x_t)$  is any function of interest. *Selection*: The particles are resampled proportionally to the  
 163 normalized weights:  $\{x_t\}_{n=1}^N \sim \text{Multinomial}(N, \text{normalized } w_t)$ ,  $\{w_t^n = 1\}_{n=1}^N$  to prevent particle  
 164 degeneracy. We refer to Chopin & Papaspiliopoulos (2020) for more details.  
 165

166 **SMC as a search algorithm for RL** Piché et al. (2019) use SMC as a search algorithm by defining  
 167 the target distribution  $p_t(\tau_t)$  over trajectories  $\tau_t = (s_0, a_0, \dots, s_t, a_t, s_{t+1}) = x_{0:t}$  (superscripted  $\tau_t^n$   
 168 to denote trajectory per particle). The target is conditioned on an optimality variable  $\mathcal{O}_{1:H}$ , such that  
 169  $p(\mathcal{O}_{1:H} | \tau_H) \propto \exp\left(\sum_{t=1}^H r_t\right)$ , following the control-as-inference (CAI) framework (see Levine,  
 170 2018), up to a horizon  $H$ . The proposal distribution is defined using a prior policy  $\pi_\theta$ , while the  
 171 target distribution incorporates the soft-optimal policy  $\mu$  and the soft-value function  $V_{\text{soft}}$ :  
 172

$$u_t(\tau_t | \tau_{t-1}) = P(s_t | s_{t-1}, a_{t-1}) \pi_\theta(a_t | s_t), \quad (6)$$

$$p_t(\tau_t | \tau_{t-1}) \propto P(s_t | s_{t-1}, a_{t-1}) \mu(a_t | s_t) \mathbb{E}_{s_{t+1}|s_t, a_t} [\exp(A_{\text{soft}}(s_t, a_t, s_{t+1}))], \quad (7)$$

$$w_t^n = w_{t-1}^n \frac{p_t(\tau_t^n | \tau_{t-1}^n)}{u_t(\tau_t^n | \tau_{t-1}^n)} \propto w_{t-1}^n \frac{\mu(a_t^n | s_t^n)}{\pi_\theta(a_t^n | s_t^n)} \mathbb{E}_{s_{t+1}^n | s_t^n, a_t^n} [\exp(A_{\text{soft}}(s_t^n, a_t^n, s_{t+1}^n))], \quad (8)$$

173 where  $A_{\text{soft}}(s_t, a_t, s_{t+1}) = r_t + V_{\text{soft}}(s_{t+1}) - \log \mathbb{E}_{s_t | s_{t-1}, a_{t-1}} V_{\text{soft}}(s_t)$ . See (Piché et al., 2019) for  
 174 derivation. We refer to this algorithm as CAI-SMC to distinguish from other variations. In the  
 175 maximum entropy setup,  $\mu$  is a uniform policy, which recovers the maximum entropy solution  
 176 (Haarnoja et al., 2018).  $V_{\text{soft}}$  is learned using a deep neural network trained with a temporal-difference  
 177 loss. Piché et al. (2019) train the policy  $\pi_\theta$  using Soft Actor Critic (Haarnoja et al., 2018). The policy  
 178 returned by CAI-SMC is only used to select actions in the environment. The model used by the  
 179 planner is learned from interactions.  
 180

181 Macfarlane et al. (2024) showed that CAI-SMC can be used as a policy improvement operator in  
 182 a manner similar to that in which MCTS is used by AZ, in their method SPO. SPO uses the SMC  
 183 planner derived by Piché et al. (2019) (CAI-SMC) with  $\mu = \pi_\theta$  which facilitates an Expectation-  
 184 Maximization framework and allows the policy to concentrate over time to the true optimal policy,  
 185 rather than the soft-optimal policy of CAI.  
 186

### 187 3 SEQUENTIAL MONTE CARLO SEARCH FOR REINFORCEMENT LEARNING

188 We begin by extending Piché et al. (2019)'s formulation of SMC as a search algorithm for RL beyond  
 189 the framework of CAI. This formulation is simpler, accepts general improvement operators  $\mathcal{I}$  and  
 190 facilitates a perspective shift from *reasoning over a distribution over trajectories* to *reasoning over the values of actions from a mixture of improved policies at the root* which we will build on in the  
 191 following sections. Similar to Piché et al. (2019), we formulate the proposal  $u_t(\tau_t)$  and target  $p_t(\tau_t)$   
 192 distributions as distributions over trajectories  $\tau_t = s_0, a_0, \dots, s_t, a_t, s_{t+1}$ . We define the proposal  
 193 distribution  $u_t(\tau_t)$  as the distribution induced by some prior policy  $\pi_\theta$ :  
 194

$$u_t(\tau_t) = \rho(s_0) \prod_{i=0}^t P(s_{i+1}|s_i, a_i) \pi_\theta(a_i|s_i) \Rightarrow u_t(\tau_t | \tau_{t-1}) = P(s_{t+1}|s_t, a_t) \pi_\theta(a_t|s_t). \quad (9)$$

195 We define the target distribution  $p_t(\tau_t)$  as the distribution induced by an improved policy  $\pi' = \mathcal{I}(\pi_\theta, Q^\pi)$  for some policy improvement operator  $\mathcal{I}$ :  
 196

$$p_t(\tau_t) = \rho(s_0) \prod_{i=0}^t P(s_{i+1}|s_i, a_i) \pi'(a_i|s_i) \Rightarrow p_t(\tau_t | \tau_{t-1}) = P(s_{t+1}|s_t, a_t) \pi'(a_t|s_t). \quad (10)$$

197 Given  $p_t(\tau_t)$  and  $u_t(\tau_t)$ , the importance sampling weights  $w_t^n$  for SMC derive as follows:  
 198

$$w_t^n = w_{t-1}^n \frac{p_t(\tau_t^n | \tau_{t-1}^n)}{u_t(\tau_t^n | \tau_{t-1}^n)} = w_{t-1}^n \frac{P(s_{t+1}^n | s_t^n, a_t^n) \pi'(a_t^n | s_t^n)}{P(s_{t+1}^n | s_t^n, a_t^n) \pi_\theta(a_t^n | s_t^n)} = w_{t-1}^n \frac{\pi'(a_t^n | s_t^n)}{\pi_\theta(a_t^n | s_t^n)} \quad (11)$$

199 In practice, the value  $Q^\pi(s, a)$  used to compute the improved policy  $\pi'$  is approximated with DNNs  
 200  $q_\phi(s, a)$  or  $r(s, a) + \gamma v_\phi(s')$  like in CAI-SMC and A/MZ. We refer to this formulation as **RL-SMC**  
 201 (Algorithm 2). Equation 11 reduces to Equation 8 for the soft-advantage operator of CAI-SMC (see  
 202 Appendix A.2 for full derivation).  
 203

204 **Policy improvement at the root** Like CAI-SMC, RL-SMC produces a policy  $\hat{\pi}_{\text{SMC}}^T$  at the root  $s_0$   
 205 after  $T$  steps with empirical occupancy counts using the particles:  
 206

$$\hat{\pi}_{\text{SMC}}^T(a|s_0) := \frac{1}{N} \sum_{n=1}^N \mathbb{1}_{\tau_T^n(a_0)=a} \approx \mathbb{P}(\tau_T(a_0) = a) =: \pi_{\text{SMC}}^T(a|s_0), \quad (12)$$

216 where  $\tau_T(a_0)$  denotes the first action in the trajectory. We verify that RL-SMC approximates policy  
 217 improvement so that it can drive an approximate policy iteration loop in a similar manner to MCTS:  
 218

219 **Theorem 1.** *For any improvement operator  $\mathcal{I}$ , search horizon  $T$ , prior policy  $\pi_\theta$ , true dynamics  
 220 model  $(P, R)$  and true evaluation  $Q^{\pi_\theta}$  RL-SMC with infinite particles is a policy improvement  
 221 operator.*

222 **Intuition** RL-SMC produces a distribution over trajectories  $p_T(\tau_T)$  from a policy that is improved  
 223 with respect to the prior policy  $\pi_\theta$  at states  $\{s_0, \dots, s_T\}$ . Since this policy is improved with respect  
 224 to the future  $\{s_0, \dots, s_{T+1}\}$ , it is of course also improved at  $s_0$ , the current state in the environment.  
 225 See Appendix A.1 for a complete proof.

226 The proof of Theorem 1 points to one of the advantages of using search for policy improvement  
 227 compared to model-free approaches. By unrolling with the model, RL-SMC produces a policy that is  
 228 improved for  $T$  consecutive time steps, in contrast to the single step of model free methods:

229 **Corollary 1.** *For any strict improvement operator  $\mathcal{I}$ , search horizon  $T$ , prior policy  $\pi_\theta$ , true dynamics  
 230 model  $(P, R)$  and true evaluation  $Q^{\pi_\theta}$  the policy produced by RL-SMC satisfies:*

$$231 \quad V^{\pi_{SMC}^T}(s_0) > V^{\pi_{SMC}^{T-1}}(s_0) > \dots > V^{\pi_{SMC}^1}(s_0) > V^{\pi_\theta}(s_0) \quad (13)$$

233 as long as  $\pi_\theta$  is not already an arg max policy with respect to  $Q^{\pi_\theta}$  at all states  $s_0, \dots, s_T$ .

235 The proof follows directly from applying strict improvement operators (improvement operators that  
 236 satisfy a strict  $>$  inequality 2 at all states unless the policy is already an arg max policy).

237 However, the root estimator  $\hat{\pi}_{SMC}^T(s_0)$  suffers from two major problems: variance that grows sharply  
 238 in  $T$  and path degeneracy (see Chopin, 2004; Chopin & Papaspiliopoulos, 2020).

240 **Large variance** The variance of SMC can scale up to polynomially with depth  $t$ , in order  $\mathcal{O}(t^\Omega)$ ,  
 241 where  $\Omega$  is the dimension of the domain of the target distribution,  $p_t(\tau_t)$  (Chopin, 2004). In RL/CAI-  
 242 SMC however the dimension of the domain  $\tau_t$  itself grows linearly with  $t$ :  $\Omega_t = d_{s,a}t$ , where  $d_{s,a}$  is  
 243 the joint dimension of the state-action space  $\mathcal{S}, \mathcal{A}$  (for example if  $s \in \mathbb{R}^5, a \in \mathbb{R}^2$  then  $d_{s,a} = 7$ ). As  
 244 a result, the variance of the estimator can increase up to super-exponentially in  $t$ :  $\mathcal{O}(t^{td_{s,a}})$ .

246 **Path degeneracy** Consecutive selection steps  $t$  are likely to concentrate all particles  $i$  to trajectories  
 247 that are associated with one root action  $a_0^i$ . Once all particles are associated with the same root action  
 248  $a_0^i$ , say at a step  $h$ , the estimator  $\hat{\pi}_{SMC}^t(a_0^i|s_0) = 1$  and zero for all other root actions  $a_0 \neq a_0^i$ .  
 249 From that point on, the estimator will not change for all depth  $t > h$ . This is problematic for two  
 250 reasons: (i) The search has no effect from  $t > h$ , and the algorithm cannot scale with additional  
 251 sequential compute (increasing  $T$ ). This is because particles will not be resampled out of trajectories  
 252 starting in action  $a_0^i$  and therefore,  $\hat{\pi}_{SMC}^t(a_0^i|s_0)$  will not change for  $t > h$ . (ii) It results in a delta  
 253 distribution policy target at the root  $s_0$  that is a crude approximation for any underlying improved  
 254 policy  $\pi_{improved}(s_0)$  but an arg max.

255 Unlike RL-SMC, MCTS treats the search problem as the problem of identifying the best action at the  
 256 root using value estimates  $Q_M(s_0, \cdot) \approx Q^{\pi_{improved}}(s_0, \cdot)$ , rather than a distribution over trajectories  
 257  $p_t(\tau_t)$ . By averaging the returns of all trajectories observed during search MCTS reduces the variance  
 258 of the root estimator  $Q_M$ . Additionally, by maintaining a value estimate for each visited action at the  
 259 root MCTS prevents the effects of path degeneracy:  $Q_M$  updates with each search step, and the policy  
 260 cannot collapse to a delta distribution, resulting in richer policy targets. This observation motivates  
 261 the next step in the design of the algorithm: a value-based perspective on RL-SMC’s search.

## 262 4 VALUE-BASED SEQUENTIAL MONTE CARLO

265 Maintaining estimates  $Q^{\pi_{SMC}^t}(s_0, a)$  in addition to a distribution over trajectories from the root can  
 266 address both of the problems caused by path degeneracy as discussed earlier: (i) The estimate  $Q^{\pi_{SMC}^t}$   
 267 does not stop updating when all particles are associated with one action at  $t = h$  and thus search  
 268 for  $t > h$  is not obsolete, allowing SMC to benefit from increased search depth. (ii) Information  
 269 is not lost about actions that have no remaining particles, and thus, target degeneracy is prevented.  
 This is similar to the idea recently proposed by de Vries et al. (2025), albeit in the guise of policy

270 log-probabilities in the framework of CAI. The value at the root  $Q^{\pi_{SMC}^t}(s_0, \cdot)$  can be approximated  
 271 using the particles:  
 272

$$273 \quad Q^{\pi_{SMC}^t}(s_0, a_0) = \mathbb{E}_{\pi_{SMC}^t} \left[ \sum_{i=0}^t \gamma^i r_i + \gamma^{t+1} V^{\pi_\theta}(s_{t+1}) \mid s_0, a_0 \right] \quad (14)$$

$$274 \quad \approx \sum_{n=1}^N w_t^n \mathbb{1}_{a_0^n = a_0} \sum_{i=0}^t \gamma^i r_i^n + \gamma^{t+1} V^{\pi_\theta}(s_{t+1}^n) := Q_t(s_0, a_0) \quad (15)$$

275 The estimator  $Q_t(s_0, a_0)$  by itself however is potentially just as high variance as  $\pi_{SMC}^t$ . Instead, we  
 276 can keep track of the *average* return observed during search, with a backpropagation step similar to  
 277 MCTS:  $\bar{Q}_t(s_0, a_0) = \frac{1}{t} \sum_{i=1}^t Q_i(s_0, a_0)$ . Whenever there are no particles associated with action  $a_0$ ,  
 278 the value  $\bar{Q}_t(s_0, a_0)$  is not updated. By mixing predictions for different steps  $Q_1, \dots, Q_t$ , any errors  
 279 that can average out now average out (see Appendix A.4 for more detail). On the other hand, although  
 280  $Q_t$  is an unbiased estimate of  $Q^{\pi_{SMC}^t}$ ,  $\bar{Q}_t$  is not. Instead,  $\bar{Q}_t$  estimates the value of a mixture of more  
 281 and more improved policies  $\pi_{SMC}^1, \dots, \pi_{SMC}^t$ . Since every policy  $\pi_{SMC}^i$  in the mixture is already  
 282 an improved policy, this is not a problem, it merely results in a value estimate of a less-improved (but  
 283 still improved) policy than  $\pi_{SMC}^T$ .  
 284

285 This value-based extension to RL-SMC can be thought of as iterating: (i) *Search*: compute importance  
 286 sampling weights to align with the improved policy  $\pi'(s_t)$ . (ii) *Backpropagation*: evaluate the returns  
 287 for each particle at states  $s_{t+1}$ , average the return across all particles associated with the same  
 288 action  $a_0$  at the root and incorporate it into the running mean  $\bar{Q}_t$ . (iii) *Expansion*: sample from the  
 289 prior-policy  $\pi_\theta(s_{t+1})$ . Due to the similarity between this three-step process and MCTS', we refer to  
 290 this algorithm as Sequential-Monte-Carlo Tree Search (**SMCTS**, summarized in Algorithm 3).  
 291

292 **Policy improvement at the root** To extract policy improvement at the root  $\pi_{improved}(s_0)$  using  
 293 the value estimates  $\bar{Q}_T(s_0, \cdot)$ , any policy improvement operator  $\mathcal{I}$  can be chosen. SMCTS returns:  
 294

$$295 \quad \pi_{improved}(s_0) = \mathcal{I}(\pi_\theta, \bar{Q})(s_0), \quad V_{search}(s_0) = \sum_{a \in A_0} \bar{Q}_T(s_0, a) \pi_{improved}(a | s_0). \quad (16)$$

296 One effect of path degeneracy remains however: all particles can still collapse to search only one root  
 297 ancestor. In addition, SMCTS does not fully leverage the insight that the search objective is policy  
 298 improvement *specifically* at the root. We address these next.  
 299

## 300 5 TWICE-SEQUENTIAL MONTE CARLO TREE SEARCH

301 One of the key observations of Danihelka et al. (2022) is that at the root of the search tree  $s_0$ , the  
 302 search budget of the algorithm is known in advance. This motivates using known-budget-optimization  
 303 algorithms such as SH (see Section 2) at the root of the search tree. By combining SH (Karnin et al.,  
 304 2013) with SMCTS, we are able to further reduce estimator variance and mitigate remaining effects  
 305 of path degeneracy at the root.  
 306

307 At each SH iteration  $i$ , SH resets the search back to the root. This results in repeated re-searching  
 308 of actions at the root. By aggregating the value predictions  $\bar{Q}_T^i$  of SMCTS across iterations  $i$ , SH  
 309 induces further lower variance estimates of the value at the root. This is similar to existing methods  
 310 to addressing variance in SMC such as *Ancestor Sampling* (Lindsten et al., 2014). Further, at each  
 311 iteration  $i$  SH reduces the number of searched actions while increasing the search budget per action.  
 312 As a result, SH minimizes the variance of the estimator for the value-maximizing actions: the actions  
 313 that are the most important for action selection and policy improvement. Finally, SH searches each  
 314 action at the root independently in parallel, which mitigates the remaining effect of path degeneracy  
 315 at the root. We formulate this Sequential-Halving Sequential-Monte-Carlo Tree Search algorithm, or  
 316 *Twice Sequential Monte Carlo Tree Search* (**TSMCTS**), below.  
 317

318 **TSMCTS** requires a number of particles  $N$ , depth budget  $T$ , and a number of starting actions to  
 319 search at the root  $m_1$ . The total search budget (number of model expansions)  $B = NT$  is then the  
 320 particle budget multiplied by the depth budget. The total number of iterations of SH is  $\log_2 m_1$ .  
 321 SH assigns a compute budget  $B_i$  per action at the root per iteration  $i = 1, \dots, \log_2 m_1$ .  $B_i$  can

324 be computed as follows:  $B_i = \frac{NT}{m_i \log_2 m_1}$ , where  $m_{i+1} = m_i/2$ ,  $i \geq 1$ . In order to preserve the  
 325 parallelizability properties of SMC we assign  $N/m_i$  particles per-action per-iteration (we assume for  
 326 simplicity that  $m_i$  divides  $N$  and otherwise round for a total particle budget of  $N$  at each iteration).  
 327 This results in the number of particles per-action per-iteration doubling every iteration:  $N_{i+1} = 2N_i$ .  
 328 To maintain the same total compute cost  $B = NT$  as SMC, at each iteration  $i$  SH searches up to  
 329 depth  $T_{SH} < T$ :

$$330 \quad T_{SH} = \frac{B_i}{N/m_i} = \frac{NT}{m_i \log_2 m_1} \frac{m_i}{N} = \frac{T}{\log_2 m_1} < T. \quad (17)$$

333 Instead of searching to the full depth  $T$ , TSMCTS searches repeatedly to a lesser depth  $T_{SH}$ , and thus  
 334 each individual estimator  $\bar{Q}_{T_{SH}}^i$  is a lower variance estimator. This results in additional reduction in  
 335 estimator variance in  $T$ , traded off against reduction in the search horizon which becomes  $T_{SH}$ .  
 336

337 At the first iteration  $i = 1$ , the set  $A_1$  of  $m_1$  actions to search are chosen as the top  $m_1$  actions  
 338 according to probabilities  $\pi_\theta(s_0)$ . To approximate sampling without replacement from the policy, in  
 339 discrete action spaces we use the Gumbel-top-k trick (Kool et al., 2019), which adds noise from the  
 340 Gumbel distribution ( $g \in \mathbb{R}^{|\mathcal{A}|} \sim \text{Gumbel}(0)$ ,  $\pi(s_0) \propto \exp(\log \pi_\theta(s_0) + g)$ ).

341 At each iteration  $i \geq 1$  TSMCTS executes SMCTS as a subroutine independently in parallel for each  
 342  $a \in A_i$ , the top  $m_i$  ( $i > 1 : m_i = \frac{m_{i-1}}{2}$ ) actions at the root according to the current improved policy:

$$344 \quad i = 1 : A_1 = \arg \text{top}(\pi(s_0), m_1), \quad i > 1 : A_i = \arg \text{top}(\mathcal{I}(\pi, Q_{SH}^{i-1})(s_0), m_i). \quad (18)$$

345 SMCTS returns the value of the improved policy at the next state for this iteration,  $V_{SMCTS}^i(s_1)$ . The  
 346 value for each action at the root  $a \in A_i$  is computed:  $Q_{SMCTS}^i(s_0, a) = r(s_0, a) + \gamma V_{SMCTS}^i(s_1)$ .  
 347 As noted above, because the search budget per action doubles each iteration,  $Q_{SMCTS}^i$  is a lower-  
 348 variance estimator than  $Q_{SMCTS}^{i-1}$  for all actions visited this iteration. To account for that we extend  
 349 the computation of the value average across iterations  $i$  to a weighted average. The average is  
 350 weighted by the "visitations" - the number of particles - to this action this iteration:  
 351

$$352 \quad \forall a \in A_i : \quad Q_{SH}^i(s_0, a) = \frac{1}{\sum_{j=1}^i N_j(a)} \sum_{j=1}^i N_j(a) Q_{SMCTS}^j(s_0, a), \quad (19)$$

355 where  $N_i(a) \geq 0$  is the number of particles assigned to root action  $a$  at iteration  $i$  and  
 356  $Q_{SMCTS}^i(s_0, a) := 0$  for root actions  $a$  that were not searched at iteration  $i$  (the term  $Q_{SMCTS}^i(s_0, a)$   
 357 will be multiplied by  $N_i(a) = 0$  for these actions and thus the actual value does not matter). In  
 358 practice, we maintain two vectors of size  $m_1$  of running sums:  
 359

$$360 \quad N^i(a) := \sum_{j=1}^i N_j(a), \quad Q_{sum}^i(s_0, a) = \sum_{j=1}^i N_j(a) Q_{SMCTS}^j(s_0, a). \quad (20)$$

363 TSMCTS returns: (i) The improved policy at the root computed using the last iteration's Q-  
 364 value:  $\pi_{improved} = \mathcal{I}(\pi, Q_{SH}^{\log_2 m_1})$ . (ii) An estimate of the value of the policy  $V_{search}(s_0) =$   
 365  $\sum_{a \in A_1} \pi_{improved}(a|s_0) Q_{SH}^{\log_2 m_1}(s_0, a)$ . These outputs are used to train the value and policy  
 366 networks in the same manner as SPO and A/MZ. That is, the improved policy  $\pi_{improved}$  is used to train  
 367 the policy  $\pi_\theta$  using cross-entropy loss. The value estimate  $V_{search}(s_0)$  is used to bootstrap value  
 368 targets to train the critic  $v_\phi$ , as in (de Vries et al., 2025). Action selection is done by sampling from the  
 369 improved policy during learning  $a \sim \pi_{improved}(s_0)$  and deterministically taking the arg max action  
 370 during evaluation  $a = \arg \max_{b \in A_1} \pi_{improved}(b|s_0)$ . We refer to Appendix B for more details.  
 371

372 A more detailed derivation of Equation 19 and discussion of the variance reduction mechanisms are  
 373 provided in Appendices A.3 and A.4 respectively. TSMCTS maintains the same space and runtime  
 374 complexity of the RL-SMC baseline (see Appendix A.5). We summarize TSMCTS in Algorithm 4.

375 **Choice of operator** The operator  $\mathcal{I}_{GMZ}$  was used by Danihelka et al. (2022) for search and policy  
 376 improvement at the root in MCTS.  $\mathcal{I}_{GMZ}$  intentionally balances between maximizing with respect to  
 377  $Q$  while minimizing the divergence from  $\pi_\theta$ , making it a natural choice for TSMCTS as well.

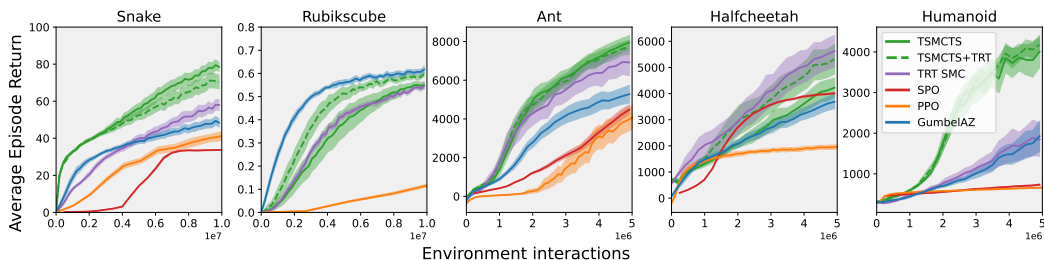
378 **6 RELATED WORK**  
 379

380 SMC has been used in RL and more generally MDP solving for a variety of purposes (see (Lazaric  
 381 et al., 2007; Hoffman et al., 2007; Le et al., 2018) for examples). Our focus in this section is on related  
 382 work in the area of SMC for search in RL. Multiple works build upon Piché et al. (2019)’s derivation  
 383 of CAI-SMC for search. Lioutas et al. (2023) extend the proposal distribution with a  $Q$  critic, to direct  
 384 the mutation step towards more promising trajectories. Macfarlane et al. (2024)’s approach of using  
 385 CAI-SMC for policy improvement and benefiting from SMC’s capacity to parallelize effectively  
 386 across particles. de Vries et al. (2025) extends the SMC search further with trust-region optimization  
 387 methods and additionally address terminal states with *revived resampling*. These advancements  
 388 are orthogonal and natural to incorporate into RL-SMC and TSMCTS (see Figure 1 in Section 7).  
 389 de Vries et al. (2025) also propose to address path degeneracy by essentially maintaining the *last*  
 390 return observed for each action at the root, thus preventing the collapse of the improved policy at the  
 391 root to a delta distribution. In contrast, SMCTS aggregates *all* returns observed for each root action  
 392 during search. This addresses path degeneracy in the same manner but acts as a reduced variance  
 393 estimator (as demonstrated in Figure 4, center, in the next section).  
 394

395 Modifications to MCTS’s classic backpropagation step, such as TD- $\lambda$  (Sutton, 1988) variations, have  
 396 been explored (Khandelwal et al., 2016). Such modifications are natural to incorporate into TSMCTS  
 397 as well, especially with the aim to further reduce estimator variance. However, these have yet to  
 398 popularize for MCTS, suggesting that they are not critical to the algorithm’s performance and we  
 399 leave their exploration in TSMCTS for future work. We include a brief summary of previous work on  
 400 parallelizing MCTS and related challenges in Appendix A.5.  
 401

402 **7 EXPERIMENTS**  
 403

404 The objective of this work is to improve SMC as a search algorithm for policy improvement in RL with  
 405 our novel method TSMCTS. To evaluate empirically that TSMCTS is a better policy improvement  
 406 operator than SMC we use the experimental setup established by Macfarlane et al. (2024) and  
 407 iterated upon by de Vries et al. (2025). This setup contains a mix of discrete and continuous control  
 408 environments from Jumanji (Bonnet et al., 2024) and Brax (Freeman et al., 2021). de Vries et al.  
 409 (2025) reduced the transition counts in evaluation to the standard in literature, and replaced one of  
 410 the sparse-reward, single-goal environments (Boxoban) to a multi-reward environment (Snake), to  
 411 increase the diversity of the environments covered in this experimental suite. We begin by comparing  
 412 a model-based agent which uses TSMCTS for policy improvement (Algorithm 1) to other popular  
 413 baselines which use search for policy improvement: **SPO** (Macfarlane et al., 2024), **TRT-SMC**  
 414 (de Vries et al., 2025) and **GumbelAZ**, an AZ agent using a modern version of MCTS (Danihelka  
 415 et al., 2022). All agents use the true dynamics model for search in the AZ manner. The SMC-based  
 416 baselines (SPO, TRT SMC, TSMCTS) are agnostic to continuous / discrete action spaces. GumbelAZ  
 417 has been extended to continuous environments in the manner of SampledMZ (Hubert et al., 2021).  
 418 We include PPO (Schulman et al., 2017) for reference performance of a popular model-free baseline.  
 419 Our implementation of all agents relies on that of de Vries et al. (2025), with the exception of SPO,  
 420 which uses the original implementation (Toledo, 2024) in the environments for which it had been  
 421 made public. As mentioned in Section 6, the contributions of de Vries et al. (2025) are for the most  
 422 part orthogonal to ours. To demonstrate that this is the case, we include a **TSMCTS + TRT** agent  
 423 which incorporates these contributions of de Vries et al. (2025) to the backbone of TSMCTS. See  
 424 Appendices B and D for additional implementation details. The results are presented in Figure 1. In  
 425 all environments the TSMCTS-based agents outperform or match all baselines.  
 426



427  
 428  
 429  
 430  
 431 Figure 1: Averaged returns vs. environment interactions. 95% Gaussian CIs across 20 seeds.

We proceed to evaluate TSMCTS as a policy improvement operator directly. In Figure 2 we compare *identical* model based agents using the exact same implementation of Algorithm 1, differing only in the search procedure used for policy improvement: **TSMCTS**, the **SMC baseline** used by Macfarlane et al. (2024) and **GumbelMCTS**. We omit TRT SMC from this comparison as its modification to SMC have been shown to be orthogonal to TSMCTS’s in Figure 1. This comparison also strengthens the connections between popular algorithmic setups of model based RL: the only difference between the GumbelMCTS agent, which is an AZ agent (GumbelAZ in Figure 1) and the SMC baseline, which is a simplified SPO agent (modified value targets, static temperature, etc.) is the search algorithm used for policy improvement. To emphasize the this connection we use the same colors for the related agents across figures. TSMCTS is overall the dominant search operator for policy improvement compared to both the SMC baseline and GumbelMCTS in these experiments.

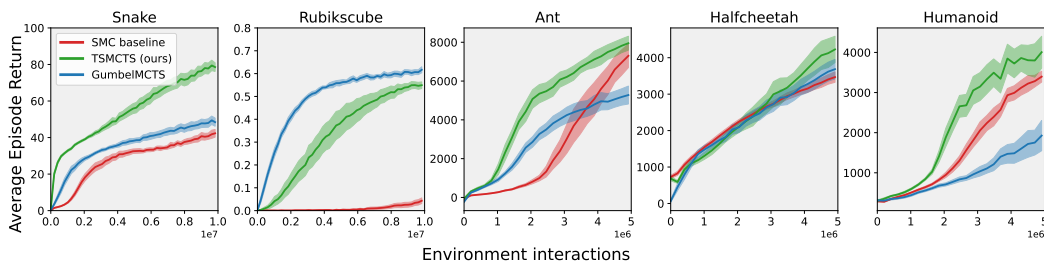


Figure 2: Averaged returns vs. environment interactions. 95% Gaussian CIs across 20 seeds.

In Figure 3 we include a reference runtime comparison between the three search algorithms. Runtime was estimated by multiplying training step with average runtime-per-step. TSMCTS induces a modest runtime increase over SMC for the same compute resources and compares very well to MCTS which has roughly twice the runtime cost as the SMC-based variants.

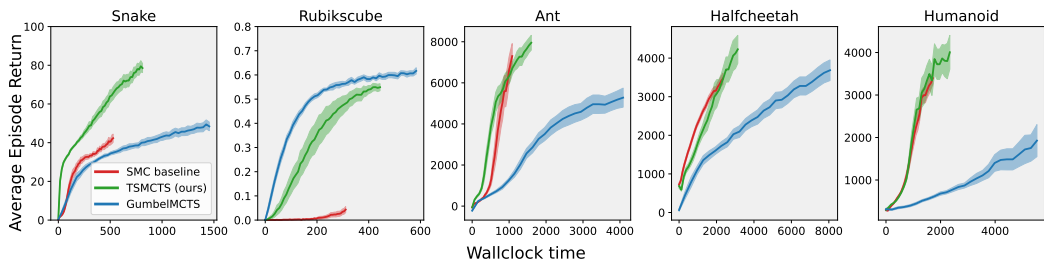


Figure 3: Averaged returns vs. runtime (seconds). Mean and 95% Gaussian CI across 20 seeds.

Next, we demonstrate empirically that TSMCTS addresses the limitations of SMC discussed in this work. In Figure 4 we plot: (i) Scaling with sequential compute (increasing depth  $T$ , left). (ii) Variance of the root estimator (center). (iii) Policy collapse at the root (target degeneracy) as a measure for path degeneracy (right).

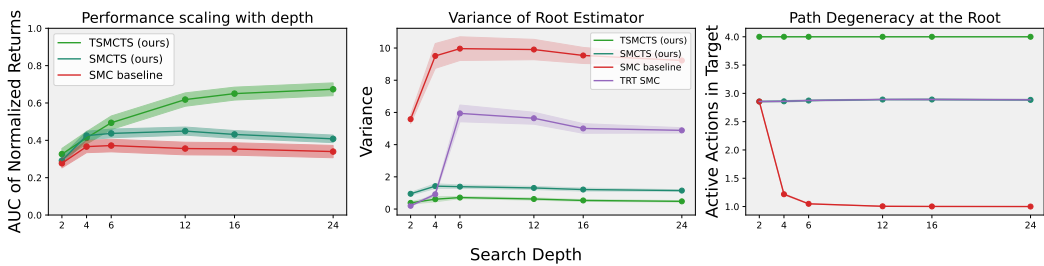


Figure 4: **Left:** Performance scaling with depth (higher is better), averaged across environments and particle budgets of 4, 8, 16. 10 seeds and 90% two-sided BCa-bootstrap intervals. **Center:** Variance of the root estimator vs. depth (lower is better). **Right:** The number of actions active in the policy target (constant - no target degeneracy - better). Center and right are averaged across states and particle budgets 4, 8, 16 and 5 seeds in Snake. Mean and 95% Gaussian CI.

We compare baseline SMC, the intermediary SMCTS and the final algorithm TSMCTS. In the variance and path degeneracy experiments we include an SMC variant which uses the mechanism proposed by de Vries et al. (2025) for mitigating path degeneracy (e.g. TRT SMC). This, to demonstrate that while this mechanism mitigates path degeneracy in the same manner as SMCTS it does not address estimator variance as well. Performance is summarized as area-under-the-curve (AUC) for the evaluation returns during training normalized across environments. The normalization is with respect to minimum and maximum AUCs observed over all agents and seeds per environment. The variance measured is over the prediction of the root estimator for each planner  $\mathbb{V}[V_{\text{search}}(s)] = \mathbb{V}[\sum_{a \in A} \pi_{\text{improved}}(a|s) Q_{\text{search}}(s, a)]$  (where  $A$  is the set of actions searched by the respective search algorithm). The variance is computed across  $L = 128$  independent calls to each planner per seed at every state in an evaluation episode after training has completed in the Snake environment, averaged across states and seeds. Target degeneracy is measured as the number of active actions in the policy target. The number of active actions at the root is averaged across the  $L$  calls to the search algorithm.

TSMCTS is the only SMC variant to successfully scale with sequential compute (Figure 4 left). TSMCTS and SMCTS have significantly reduced estimator variance compared to the other SMC variants and TSMCTS’s is significantly reduced compared to SMCTS’s (Figure 4 center). All variants other than baseline address policy collapse at the root. TRT SMC and SMCTS however are limited by the entropy of the policy: the policy has high probability for only two actions in most states despite the size of the action space being 4 in this environment and thus only two actions are searched. TSMCTS on the other hand searches a constant  $m_1 = 4$  actions, irrespective of the prior policy.

We investigate the effect of the hyperparameter  $m_1$  of TSMCTS on the performance of the agent in Figures 5 in Appendix C. The effect appears overall marginal for sufficiently large  $m_1 \geq 4$ .

## 8 CONCLUSIONS

We presented Twice Sequential Monte Carlo Tree Search (TSMCTS), a search algorithm based in Sequential Monte Carlo (SMC) for action selection and policy optimization in Reinforcement Learning (RL). TSMCTS builds upon our formulation of SMC for search in RL which extends prior work (Piché et al., 2019) beyond the framework of Control As Inference (see Levine, 2018). TSMCTS harnesses mechanisms from Monte Carlo Tree Search (Świechowski et al., 2023) and Sequential Halving (Karnin et al., 2013) to mitigate the high estimator variance and path degeneracy problems of SMC, while maintaining SMC’s beneficial runtime and space complexity properties. In experiments across discrete and continuous environments TSMCTS outperforms the SMC baseline as well as a popular modern version of MCTS (GumbelMCTS, Danihelka et al., 2022). In contrast to the SMC baseline, TSMCTS demonstrates lower estimator variance, mitigates the effects of path degeneracy at the root and scales favorably with sequential compute.

## REPRODUCIBILITY STATEMENT

Special care was taken to support reproducibility. Proofs and more detailed discussion of theoretical results are provided in Appendix A. Implementation details are described in Appendix B. Hyperparameters are listed in Appendix D. The codebase will be made public upon acceptance.

## LLM USAGE

LLMs were used in a minor role, to improve a small number of text paragraphs and for additional, supplementary, retrieval and discovery of related work.

## REFERENCES

Richard Bellman. A Markovian Decision Process. *Journal of Mathematics and Mechanics*, 6(5): 679–684, 1957.

Clément Bonnet, Daniel Luo, Donal John Byrne, Shikha Surana, Sasha Abramowitz, Paul Duckworth, Vincent Coyette, Laurence Illing Midgley, Elshadai Tegegn, Tristan Kalloniatis, Omayma Mahjoub,

540 Matthew Macfarlane, Andries Petrus Smit, Nathan Grinsztajn, Raphael Boige, Cemlyn Neil Waters,  
 541 Mohamed Ali Ali Mimouni, Ulrich Armel Mbou Sob, Ruan John de Kock, Siddarth Singh, Daniel  
 542 Furelos-Blanco, Victor Le, Arnu Pretorius, and Alexandre Laterre. Jumanji: a diverse suite of  
 543 scalable reinforcement learning environments in JAX. In *The Twelfth International Conference on  
 544 Learning Representations*, 2024.

545 James Bradbury, Roy Frostig, Peter Hawkins, Matthew James Johnson, Chris Leary, Dougal  
 546 Maclaurin, George Necula, Adam Paszke, Jake VanderPlas, Skye Wanderman-Milne, and  
 547 Qiao Zhang. JAX: composable transformations of Python+NumPy programs, 2018. URL  
 548 <http://github.com/jax-ml/jax>.

549 Alan Chan, Hugo Silva, Sungsu Lim, Tadashi Kozuno, A. Rupam Mahmood, and Martha White.  
 550 Greedification Operators for Policy Optimization: Investigating Forward and Reverse KL Diver-  
 551 gences. *Journal of Machine Learning Research*, 23(253):1–79, 2022.

552 Guillaume Chaslot, Mark H. M. Winands, and H. Jaap van den Herik. Parallel Monte-Carlo Tree  
 553 Search. In *Computers and Games, CG 2008*, volume 5131 of *Lecture Notes in Computer Science*,  
 554 pp. 60–71. Springer, Berlin, Heidelberg, 2008. doi: 10.1007/978-3-540-87608-3\_6.

555 Nicolas Chopin. Central Limit Theorem for Sequential Monte Carlo Methods and its Ap-  
 556 plication to Bayesian Inference. *The Annals of Statistics*, 32(6):2385–2411, 2004. doi:  
 557 10.1214/009053604000000698.

558 Nicolas Chopin and Omiros Papaspiliopoulos. *An Introduction to Sequential Monte Carlo*. Springer  
 559 Series in Statistics. Springer, Cham, 1st edition, 2020. doi: 10.1007/978-3-030-47845-2.

560 Ivo Danihelka, Arthur Guez, Julian Schrittwieser, and David Silver. Policy improvement by planning  
 561 with Gumbel. In *The Tenth International Conference on Learning Representations*, 2022.

562 Joery A. de Vries, Jinke He, Yaniv Oren, and Matthijs T. J. Spaan. Trust-Region Twisted Policy  
 563 Improvement. In *Forty-second International Conference on Machine Learning*, 2025.

564 DeepMind, Igor Babuschkin, Kate Baumli, Alison Bell, Surya Bhupatiraju, Jake Bruce, Peter  
 565 Buchlovsky, David Budden, Trevor Cai, Aidan Clark, Ivo Danihelka, Antoine Dedieu, Clau-  
 566 dio Fantacci, Jonathan Godwin, Chris Jones, Ross Hemsley, Tom Hennigan, Matteo Hessel,  
 567 Shaobo Hou, Steven Kapturowski, Thomas Keck, Iurii Kemaev, Michael King, Markus Kunesch,  
 568 Lena Martens, Hamza Merzic, Vladimir Mikulik, Tamara Norman, George Papamakarios, John  
 569 Quan, Roman Ring, Francisco Ruiz, Alvaro Sanchez, Laurent Sartran, Rosalia Schneider,  
 570 Eren Sezener, Stephen Spencer, Srivatsan Srinivasan, Miloš Stanojević, Wojciech Stokowiec,  
 571 Luyu Wang, Guangyao Zhou, and Fabio Viola. The DeepMind JAX Ecosystem, 2020. URL  
 572 <https://github.com/google-deepmind>.

573 Alhussein Fawzi, Matej Balog, Aja Huang, Thomas Hubert, Bernardino Romera-Paredes, Mo-  
 574 hammadamin Barekatain, Alexander Novikov, Francisco J. R. Ruiz, Julian Schrittwieser, Grze-  
 575 gorz Swirszcz, David Silver, Demis Hassabis, and Pushmeet Kohli. Discovering faster matrix  
 576 multiplication algorithms with reinforcement learning. *Nature*, 610(7930):47–53, 2022. doi:  
 577 10.1038/s41586-022-05172-4.

578 C. Daniel Freeman, Erik Frey, Anton Raichuk, Sertan Girgin, Igor Mordatch, and Olivier Bachem.  
 579 Brax - A Differentiable Physics Engine for Large Scale Rigid Body Simulation. In *Thirty-fifth  
 580 Conference on Neural Information Processing Systems Datasets and Benchmarks Track (Round 1)*,  
 581 2021.

582 Stuart Geman, Elie Bienenstock, and René Doursat. Neural Networks and the Bias/Variance Dilemma.  
 583 *Neural Computation*, 4(1):1–58, 1992. doi: 10.1162/neco.1992.4.1.1.

584 Jean-Bastien Grill, Florent Altché, Yunhao Tang, Thomas Hubert, Michal Valko, Ioannis Antonoglou,  
 585 and Remi Munos. Monte-Carlo Tree Search as Regularized Policy Optimization. In *Proceedings  
 586 of the 37th International Conference on Machine Learning*, volume 119, pp. 3769–3778. PMLR,  
 587 2020.

588 Tuomas Haarnoja, Aurick Zhou, Pieter Abbeel, and Sergey Levine. Soft Actor-Critic: Off-Policy  
 589 Maximum Entropy Deep Reinforcement Learning with a Stochastic Actor. In *Proceedings of the  
 590 35th International Conference on Machine Learning*, volume 80, pp. 1861–1870. PMLR, 2018.

594 Matt Hoffman, Arnaud Doucet, Nando De Freitas, and Ajay Jasra. On solving general state-space  
 595 sequential decision problems using inference algorithms. Technical report, Technical Report  
 596 TR-2007-04, University of British Columbia, Computer Science, 2007.

597

598 Thomas Hubert, Julian Schrittwieser, Ioannis Antonoglou, Mohammadamin Barekatain, Simon  
 599 Schmitt, and David Silver. Learning and Planning in Complex Action Spaces. In *Proceedings  
 600 of the 38th International Conference on Machine Learning*, volume 139, pp. 4476–4486. PMLR,  
 2021.

601

602 Zahar Karnin, Tomer Koren, and Oren Somekh. Almost Optimal Exploration in Multi-Armed  
 603 Bandits. In *Proceedings of the 30th International Conference on Machine Learning*, volume 28,  
 604 pp. 1238–1246. PMLR, 2013.

605

606 Piyush Khandelwal, Elad Liebman, Scott Niekum, and Peter Stone. On the Analysis of Com-  
 607 plex Backup Strategies in Monte Carlo Tree Search. In *Proceedings of The 33rd International  
 608 Conference on Machine Learning*, volume 48, pp. 1319–1328. PMLR, 2016.

609

610 Wouter Kool, Herke Van Hoof, and Max Welling. Stochastic Beams and Where To Find Them: The  
 611 Gumbel-Top-k Trick for Sampling Sequences Without Replacement. In *Proceedings of the 36th  
 612 International Conference on Machine Learning*, volume 97, pp. 3499–3508. PMLR, 2019.

613

614 Alessandro Lazaric, Marcello Restelli, and Andrea Bonarini. Reinforcement Learning in continuous  
 615 action spaces through Sequential Monte Carlo methods. In John C. Platt, Daphne Koller, Yoram  
 616 Singer, and Sam T. Roweis (eds.), *Advances in Neural Information Processing Systems 20*, 2007.

617

618 Tuan Anh Le, Maximilian Igl, Tom Rainforth, Tom Jin, and Frank Wood. Auto-encoding sequential  
 619 monte carlo. *The Sixth International Conference on Learning Representations*, 2018.

620

621 Sergey Levine. Reinforcement Learning and Control as Probabilistic Inference: Tutorial and Review.  
 622 arXiv:1805.00909, 2018.

623

624 Fredrik Lindsten, Michael I Jordan, and Thomas B Schön. Particle Gibbs with ancestor sampling.  
 625 *The Journal of Machine Learning Research*, 15(1):2145–2184, 2014.

626

627 Vasileios Lioutas, Jonathan Wilder Lavington, Justice Sefas, Matthew Niedoba, Yunpeng Liu, Berend  
 628 Zwartsenberg, Setareh Dabiri, Frank Wood, and Adam Scibior. Critic Sequential Monte Carlo. In  
 629 *International Conference on Learning Representations*, 2023.

630

631 Anji Liu, Jianshu Chen, Mingze Yu, Yu Zhai, Xuewen Zhou, and Ji Liu. Watch the Unobserved: A  
 632 Simple Approach to Parallelizing Monte Carlo Tree Search. In *The Eighth International Conference  
 633 on Learning Representations*, 2020.

634

635 Ilya Loshchilov and Frank Hutter. Decoupled Weight Decay Regularization. In *The Seventh  
 636 International Conference on Learning Representations*, 2019.

637

638 Matthew Macfarlane, Edan Toledo, Donal John Byrne, Paul Duckworth, and Alexandre Laterre. SPO:  
 639 Sequential Monte Carlo Policy Optimisation. In *The Thirty-eighth Annual Conference on Neural  
 640 Information Processing Systems*, 2024.

641

642 Daniel J. Mankowitz, Andrea Michi, Anton Zhernov, Marco Gelmi, Marco Selvi, Cosmin Paduraru,  
 643 Edouard Leurent, Shariq Iqbal, Jean-Baptiste Lespiau, Alex Ahern, Thomas Koppe, Kevin Millikin,  
 644 Stephen Gaffney, Sophie Elster, Jackson Broshear, Chris Gamble, Kieran Milan, Robert Tung,  
 645 Minjae Hwang, Taylan Cemgil, Mohammadamin Barekatain, Yujia Li, Amol Mandhane, Thomas  
 Hubert, Julian Schrittwieser, Demis Hassabis, Pushmeet Kohli, Martin Riedmiller, Oriol Vinyals,  
 and David Silver. Faster sorting algorithms discovered using deep reinforcement learning. *Nature*,  
 646 618(7964):257–263, 2023. doi: 10.1038/s41586-023-06004-9.

647

648 Yaniv Oren, Viliam Vadocz, Matthijs T. J. Spaan, and Wendelin Boehmer. Epistemic Monte Carlo  
 649 Tree Search. In *The Thirteenth International Conference on Learning Representations*, 2025a.

650

651 Yaniv Oren, Moritz A Zanger, Pascal R Van der Vaart, Mustafa Mert Çelikok, Matthijs TJ Spaan,  
 652 and Wendelin Boehmer. Value Improved Actor Critic Algorithms. In *The Thirty-ninth Annual  
 653 Conference on Neural Information Processing Systems*, 2025b.

648 Alexandre Piché, Valentin Thomas, Cyril Ibrahim, Yoshua Bengio, and Chris Pal. Probabilistic  
 649 Planning with Sequential Monte Carlo methods. In *International Conference on Learning Repre-*  
 650 *sentations*, 2019.

651 Julian Schrittwieser, Ioannis Antonoglou, Thomas Hubert, Karen Simonyan, Laurent Sifre, Simon  
 652 Schmitt, Arthur Guez, Edward Lockhart, Demis Hassabis, Thore Graepel, Timothy Lillicrap, and  
 653 David Silver. Mastering Atari, Go, chess and shogi by planning with a learned model. *Nature*, 588  
 654 (7839):604–609, 2020. doi: 10.1038/s41586-020-03051-4.

655 John Schulman, Filip Wolski, Prafulla Dhariwal, Alec Radford, and Oleg Klimov. Proximal Policy  
 656 Optimization Algorithms. arXiv:1707.06347, 2017.

657 David Silver, Aja Huang, Chris J. Maddison, Arthur Guez, Laurent Sifre, George van den Driessche,  
 658 Julian Schrittwieser, Ioannis Antonoglou, Veda Panneershelvam, Marc Lanctot, Sander Dieleman,  
 659 Dominik Grewe, John Nham, Nal Kalchbrenner, Ilya Sutskever, Timothy Lillicrap, Madeleine  
 660 Leach, Koray Kavukcuoglu, Thore Graepel, and Demis Hassabis. Mastering the game of Go  
 661 with deep neural networks and tree search. *Nature*, 529(7587):484–489, 2016. doi: 10.1038/  
 662 nature16961.

663 David Silver, Thomas Hubert, Julian Schrittwieser, Ioannis Antonoglou, Matthew Lai, Arthur  
 664 Guez, Marc Lanctot, Laurent Sifre, Dharshan Kumaran, Thore Graepel, Timothy Lillicrap, Karen  
 665 Simonyan, and Demis Hassabis. A general reinforcement learning algorithm that masters chess,  
 666 shogi, and Go through self-play. *Science*, 362(6419):1140–1144, 2018. doi: 10.1126/science.  
 667 aar6404.

668 Richard S. Sutton. Learning to predict by the methods of temporal differences. *Machine Learning*, 3  
 669 (1):9–44, 1988. doi: 10.1007/BF00115009.

670 Richard S. Sutton and Andrew G. Barto. *Reinforcement Learning: An Introduction*. A Bradford  
 671 Book, 2nd edition, 2018.

672 Edan Toledo. Stoix: Distributed single-agent reinforcement learning end-to-end in jax, April 2024.  
 673 URL <https://github.com/EdanToledo/Stoix>.

674 Maciej Świechowski, Konrad Godlewski, Bartosz Sawicki, and Jacek Mańdziuk. Monte Carlo Tree  
 675 Search: a review of recent modifications and applications. *Artificial Intelligence Review*, 56(3):  
 676 2497–2562, 2023. doi: 10.1007/s10462-022-10228-y.

## 681 A THEORETICAL RESULTS

### 684 A.1 RL-SMC IS A POLICY IMPROVEMENT OPERATOR

686 *Proof.* Given exact evaluation  $Q^\pi$ , true environment model  $P, r$ , a starting state  $s_0$  and infinitely  
 687 many particles  $N \rightarrow \infty$ , the SMC target policy at final step  $T$  produces the following distribution  
 688 over trajectories:

$$689 p(\tau_T) = p(s_0, a_0, \dots, s_T, a_T, s_{T+1}) = \prod_{i=0}^T P(s_{i+1}|s_i, a_i) \pi'(a_i|s_i) \quad (21)$$

691 The distribution  $p(\tau_T)$  is equivalent to the distribution induced by following the policy  $\pi'$  for all  
 692 states  $s_{0,\dots,T}$ , and for all other states following  $\pi$ , by definition. We call this policy  $\pi_{SMC}$ . We have:

$$694 V^\pi(s_0) \leq \mathbb{E}_{\pi'}[Q^\pi(s_0, a_0)] \quad (22)$$

$$695 = \mathbb{E}_{\pi', P}[r_0 + \gamma V^\pi(s_1)] \quad (23)$$

$$696 \leq \mathbb{E}_{\pi', P}[r_0 + \gamma Q^\pi(s_1, a_1)] \quad (24)$$

$$698 \leq \mathbb{E}_{\pi', P}[r_0 + \gamma r_1 + \gamma^2 Q^\pi(s_2, a_2)] \quad (25)$$

$$699 \leq \dots \quad (26)$$

$$700 \leq \mathbb{E}_{\pi', P}[r_0 + \dots + \gamma^{T-1} r_{T-1} + \gamma^T Q^\pi(s_T, a_T)] \quad (27)$$

$$701 = V^{\pi_{SMC}}(s_0) \quad (28)$$

Equation 22 holds by definition of  $\pi'$  produced from an improvement operator. Note that actions  $a_0, a_1, a_2, \dots$  are all sampled from  $\pi'(s_1), \dots$  respectively, as the expectation is with respect to  $\pi'$  at all steps. Equation 24 holds because  $\mathbb{E}_{\pi'} Q^{\pi}(s_2, a) \geq V(s_2)$ , by definition of  $\pi'$ . Equation 25 is the two-step expansion following the same argumentation, and respectively Equation 27 is the multi-step expansion, which is the definition of the value of the policy  $\pi_{SMC}$ .

□

## A.2 DERIVING CAI-SMC IN RL-SMC

The importance sampling weights of CAI-SMC derive as follows (see the work of Piché et al. (2019)):

$$p_t(\tau_t | \tau_{t-1}) = P(s_t | s_{t-1}, a_{t-1}) \pi_\theta(a_t | s_t), \quad (29)$$

$$p_t(\tau_t | \tau_{t-1}) \propto P(s_t | s_{t-1}, a_{t-1}) \mu(a_t | s_t) \mathbb{E}_{s_{t+1} | s_t, a_t} [\exp(A_{\text{soft}}(s_t, a_t))], \quad (30)$$

$$w_t^n = w_{t-1}^n \frac{p_t(\tau_t^n | \tau_{t-1}^n)}{u_t(\tau_t^n | \tau_{t-1}^n)} \propto w_{t-1}^n \frac{\mu(a_t^n | s_t^n)}{\pi_\theta(a_t^n | s_t^n)} \mathbb{E}_{s_{t+1}^n | s_t^n, a_t^n} [\exp(A_{\text{soft}}(s_t^n, a_t^n, s_{t+1}^n))], \quad (31)$$

Denote:

$$\pi'(a_t^n | s_t^n) = \mu(a_t^n | s_t^n) \mathbb{E}_{s_{t+1}^n | s_t^n, a_t^n} [\exp(A_{\text{soft}}(s_t^n, a_t^n, s_{t+1}^n))] \quad (32)$$

Where  $\pi'$  here is the posterior probability of CAI's graphical model, or the optimal soft-policy (Piché et al., 2019):

$$\pi'(a_t^n | s_t^n) = \mu(a_t^n | s_t^n) \mathbb{E}_{s_{t+1}^n | s_t^n, a_t^n} [\exp(A_{\text{soft}}(s_t^n, a_t^n, s_{t+1}^n))] \quad (33)$$

$$= \mu(a_t | s_t) \exp[\ln p(O_{t:T} | s_t, a_t) - \ln p(O_{t:T} | s_t)] \quad (34)$$

$$= p(a_t | s_t) p(O_{t:T} | s_t, a_t) / p(O_{t:T} | s_t) \quad (35)$$

$$= p(a_t | s_t, O_{t:T}) \quad (36)$$

We have:

$$w_t^n = \propto w_{t-1}^n \frac{\mu(a_t^n | s_t^n)}{\pi_\theta(a_t^n | s_t^n)} \mathbb{E}_{s_{t+1}^n | s_t^n, a_t^n} [\exp(A_{\text{soft}}(s_t^n, a_t^n, s_{t+1}^n))] = w_{t-1}^n \frac{\pi'(a_t^n | s_t^n)}{\pi_\theta(a_t^n | s_t^n)} \quad (37)$$

Which recovers RL-SMC.

## A.3 DERIVING THE VALUE UPDATE IN TSMCTS

In MCTS, the value  $V_N(s_t)$  at each node  $s_t$  equals the average of all returns  $\frac{1}{N} \sum_{i=1}^N \sum_{k=0}^{T-1} \gamma^k r_{t+k}^i + \gamma^T v_\phi(s_{t+T}^i)$  observed through this node. This is because the variance of the estimator is expected to reduce with  $1/N$ , the number of visitations. This also holds in SMC, where for large  $N$ , the error behaves approximately Gaussian with variance proportional to  $1/N$  (Chopin, 2004). For this reason, we rely on the same idea in TSMCTS.

At each iteration  $i$  of TSMCTS the value estimate  $Q_{SMCTS}^i(s_0, a)$  was computed using  $N(i, a)$  particles per action, and thus, the contribution of this value estimate to the total average should be  $N(i, a)$ .

Equation 19 (provided below again for readability) formulates exactly this weighted average: it sums across the total number of iterations  $\log_2 m_1$ . For each iteration, it multiplies  $Q_{SMCTS}^i(s_0, a)$  by the weight  $N(i, a)$ . Finally, it normalizes the sum by  $\sum_{i=1}^{\log_2 m_1} N(i, a)$ :

$$\forall a \in M_1 : Q_{SH}^i(s, a) = \frac{1}{\sum_{i=1}^{\log_2 m_1} N(i, a)} \sum_{i=1}^{\log_2 m_1} N(i, a) Q_{SMCTS}^i(s, a)$$

## A.4 VARIANCE REDUCTION

Throughout this work, we describe different mechanisms that reduce variance in TSMCTS compared to the SMC framework TSMCTS is built upon. In this section we will describe and motivate each mechanism in more detail. We begin with an overall motivation for variance minimization.

756 Variance minimization is a fundamental objective in statistical estimation, as the quality of an  
 757 estimator is typically assessed through its mean squared error (MSE) (Geman et al., 1992). The MSE  
 758 admits a standard decomposition into the squared bias and the variance,  
 759

$$\text{MSE} = \text{Bias}^2 + \text{Var}.$$

760 While bias captures systematic deviation from the true quantity, variance reflects the sensitivity of  
 761 the estimator to fluctuations in the data. Minimizing variance - without changing the bias - therefor  
 762 reduces to minimizing estimation error. We proceed to describe each variance-reducing mechanism  
 763 in chronological order.  
 764

765 **Backpropagation in SMCTS** The running means  $\bar{Q}_t(s_0, a_0)$  maintained through backpropagation  
 766 in SMCTS decompose into:  
 767

$$\bar{Q}_t(s_0, a_0) = \frac{1}{t} \sum_{i=t}^t Q_i(s_0, a_0) = \sum_{i=1}^N w_t^i \mathbb{1}_{a_0^{(i)}=a_0} \sum_{j=0}^t \gamma^j r_j^i + \gamma^{t+1} V^{\pi_\theta}(s_{t+1}^i). \quad (38)$$

770  $\bar{Q}_t(s_0, a_0)$  is a reduced variance estimator compared to  $Q_t$  for two reasons.  
 771

772 (i) Consider the bootstrapped return:  
 773

$$Q_t(s_0, a_0) = \sum_{j=0}^t \gamma^j r_j^i + \gamma^{t+1} V^{\pi_\theta}(s_{t+1}^i). \quad (39)$$

775 For any  $h < t$ , the estimator  $Q_h(s_0, a_0)$  terminates earlier and bootstraps from  $V^{\pi_\theta}$  sooner. Since  
 776 extending the horizon from  $h$  to  $t$  replaces a single (deterministic) bootstrap term with additional  
 777 random rewards and transitions, it introduces extra stochasticity. Consequently,  $\text{Var}(Q_h(s_0, a_0)) <$   
 778  $\text{Var}(Q_t(s_0, a_0))$ , reflecting the classical result that Monte Carlo returns (large  $t$ ) have higher variance  
 779 than temporally shorter, bootstrapped estimates (small  $h$ ) (Sutton & Barto, 2018).  
 780

781 (ii) Let us assume for a moment the policy, transition dynamics and reward are all deterministic.  
 782 Any errors in the value prediction  $v_\phi$  that are I.I.D. will average out in the empirical average  
 783  $\frac{1}{N} \sum_{t=1}^N \sum_{i=0}^t \gamma^i r_i + v_\phi(s_{t+1})$  where  $s_i = P(s_{i-1}, \pi(s_{i-1}))$ . For that reason mixing different  
 784 length bootstrapped returns can result in reduced variance estimates compared to any individual  
 785 bootstrapped return even when the dynamics and rewards are deterministic.  
 786

787 **Repeatedly searching the same actions from the root in TSMCTS** At each iteration  $i$ , TSMCTS  
 788 searches a set of actions  $A_i \subset A_{i-1}$ . Since the actions are searched independently again from the  
 789 root, we have  $\text{Var}(Q_{SH}^i) < \text{Var}(Q_{SMCTS}^i)$ . That is, the average *across* the value estimates of  
 790 independent iterations is a lower variance estimate of the true value compared to each individual  
 791 estimate, for the same reasoning as above.  
 792

793 **Increasing particle budget per searched action at the root in TSMCTS** Under standard as-  
 794 sumptions, increasing the number of particles in SMC algorithms reduces variance because the  
 795 particle system provides an empirical average, and the variance of such Monte Carlo estimates  
 796 decreases proportionally to the number of particles  $1/N$ , where  $N$  is the number of particles (Chopin  
 797 & Papaspiliopoulos, 2020).  
 798

799 **Searching for a shorter horizon** TSMCTS trades off the depth of the search  $T_{SH} < T$  for repeated  
 800 search from the root. Reducing the depth of the search has two main effects: (i) It reduces the number  
 801 of consecutive improvement (or search) steps. In a manner of speaking, the resulting policy is "less  
 802 improved". (ii) It results in a lower variance estimator, as the variance grows in  $t$  and  $T_{SH} < T$ .  
 803

## 804 A.5 COMPLEXITY ANALYSIS

805 We include a brief runtime and space complexity analysis for MCTS and RL-SMC.  
 806

807 **MCTS complexity** For a search budget  $B$ , MCTS conducts  $B$  iterations. At each iteration  $i$ , MCTS  
 808 conducts  $d_i \leq B$  search steps, one expansion step, and then  $d_i \leq B$  backpropagation steps along the  
 809 nodes in the trajectory.  $d_i$  denotes the depth of the leaf at step  $i$ . We can therefore bound the runtime  
 810 complexity by  $\mathcal{O}(B(B + B + 1)) = \mathcal{O}(B^2)$  operations. In regards to space complexity, MCTS  
 811 construct a tree of size  $B$ , so the space required is of complexity  $\mathcal{O}(B)$ .  
 812

810 **RL-SMC complexity** For  $N$  particles and a depth  $T$ , the search budget of RL-SMC totals  $NT = B$ .  
 811 Assuming that  $N$  particles operate in parallel the (sequential) runtime complexity is  $\mathcal{O}(T) \leq \mathcal{O}(B) <$   
 812  $\mathcal{O}(B^2)$  operations. In terms of space, RL-SMC maintains only statistics about each particle, resulting  
 813 in space complexity of  $\mathcal{O}(N) \leq \mathcal{O}(B)$ . Since RL-SMC is merely a generalization of Piché et al.  
 814 (2019)'s CAI-SMC, we conclude that CAI-SMC has the same space and runtime complexity.  
 815

816 **SMCTS complexity** For  $N$  particles and a depth  $T$ , the search budget of SMCTS totals  $NT = B$ .  
 817 At each step  $i$ , SMCTS conducts a constant number of additional operation: one running sum is  
 818 maintained for each particle, and one running sum is maintained for each searched action at the  
 819 root. As a result, SMCTS maintains the same (sequential) runtime complexity of RL-SMC of  
 820  $\mathcal{O}(T) < \mathcal{O}(B^2)$ . SMCTS maintains statistics about  $N$  particles, and also statistics about  $M \leq N$   
 821 searched actions at the root. This results in space complexity of  $\mathcal{O}(2N) = \mathcal{O}(N) \leq \mathcal{O}(B)$ , the same  
 822 space complexity as RL-SMC.  
 823

824 **TSMCTS complexity** For  $N$  particles and a depth  $T$ , the search budget of SMCTS totals  $NT = B$ .  
 825 TSMCTS divides this budget across  $\log_2 m_1$  iterations. At each iteration, TSMCTS executes  
 826  $T / \log_2 m_1$  steps, resulting in runtime complexity of  $\mathcal{O}(\log_2 m_1 \frac{T}{\log_2 m_1}) = \mathcal{O}(T) < \mathcal{O}(B^2)$ , the  
 827 same as SMCTS and RL-SMC. In terms of space complexity, TSMCTS maintains statistics over  
 828  $N$  particles, and  $m_1 \leq N$  searched actions at the root, resulting in the same space complexity as  
 829 RL-SMC and SMCTS,  $\mathcal{O}(2N) = \mathcal{O}(N) \leq \mathcal{O}(B)$ .  
 830

831 **Parallelizing MCTS** Approaches to parallelize MCTS exist (Chaslot et al., 2008). These range  
 832 from running *leaf parallelization* which performs multiple independent rollouts from the same newly  
 833 expanded leaf node, improving evaluation accuracy but not accelerating tree growth. This of course  
 834 is not applicable with modern MCTS methods which use a value DNN to expand leaves. *Search*  
 835 *parallelization* runs MCTS in parallel across multiple states in multiple environments in parallel.  
 836 This is the current norm for JAX based implementations, such as by DeepMind et al. (2020). *Root*  
 837 *parallelization* launches multiple independent MCTS instances — each constructing its own search  
 838 tree — and aggregates root-level statistics. This is in direct competition over resources with *search*  
 839 *parallelization*. Since it runs multiple trees for the same state, it reduces the number of independent  
 840 states that can be searched in parallel, and thus slows down data gathering (number of environment  
 841 interactions per search steps). *Tree parallelization* is the most akin to the parallelization of SMC: it  
 842 shares a single MCTS tree among multiple workers, requiring synchronization mechanisms—such as  
 843 local mutexes and virtual loss—to maintain consistency and avoid redundant exploration. Overall,  
 844 this contrasts very clearly with the ease at which SMC parallelizes. In SMC one can simply increase  
 845 the number of particles  $N$ .  
 846

847 **A note on complexity in practice** It is unlikely that all operations will have the same compute cost  
 848 in practice. In search algorithms that use DNNs, it is often useful to think of two separate operation  
 849 costs: model interactions, and DNN forward passes. Either of the two can often be the compute  
 850 bottleneck, depending on the choice of model, DNN architecture, hardware etc. This motivates an  
 851 equating for compute estimated in number of model expansions / DNN forward passes which is  $B$   
 852 for MCTS and  $NT$  for SMC, which is why we as well as previous work opted to compare MCTS  
 853 and SMC variants with budgets  $B = NT$ .  
 854

## 855 B IMPLEMENTATION DETAILS

856 **Targets and losses** Our implementation for all search-based agents uses a  $v_\phi$  critic and a prior  
 857 policy  $\pi_\theta$ . The value and policy are trained with the following losses:  
 858

$$\mathcal{L}(\theta) = \mathbb{E}_{(s_t, a_t, \pi_t) \sim \mathcal{D}_{(n)}} [-\mathbb{E}_{a \sim \pi_t} \ln \pi_\theta(a|s_t) - c_{ent} \mathcal{H}[\pi_\theta(a|s_t)]], \quad (40)$$

$$\mathcal{L}(\phi) = \mathbb{E}_{(s_t, a_t, v_t) \sim \mathcal{D}_{(n)}} [(v_t - v_\phi(s_t))^2]. \quad (41)$$

859  $\pi_t$  is the policy target for state  $s_t$  which is the policy  $\pi_{improved}$  returned by the planner (be it SMC,  
 860 SMCTS, TSMCTS or MCTS).  $v_t$  is the value target for state  $s_t$  which is computed using TD- $\lambda$  with  
 861 bootstraps  $V_{search}$  returned by the planner.  $\mathcal{H}[\pi_\theta] = -\mathbb{E}_{\pi_\theta} \ln \pi_\theta$  is an entropy penalty for the policy.  
 862  $\mathcal{D}_{(n)}$  is the replay buffer for iteration  $n$ .  
 863

**The training loop** The RL training setup follows the popular approach in JAX, which gathers interaction trajectories of length *unroll length*  $L$  for a *batch size*  $B$  in parallel, resulting in a total replay buffer of size  $LB$  per episode. The agent is then trained for  $K$  *SGD update steps* with *SGD minibatch size* (see hyperparameters in Table 1) and the above losses. Following that, the agent proceeds to gather additional data of size  $LB$ . The AdamW optimizer (Loshchilov & Hutter, 2019) was used with an  $l_2$  penalty of  $10^{-6}$  and a learning rate of  $3 \cdot 10^{-3}$ . Gradients were clipped using a max absolute value of 10 and a global norm limit of 10.

**Discrete vs. continuous action spaces** The same losses are used to train the value and policy networks, irrespective of the type of action space. In continuous environments, the policy is a Gaussian policy, predicting mean and variance. In discrete environments, the policy is trained to predict the log-probabilities for each action in the action space, as is standard, using the empirical cross entropy loss  $\mathcal{L}(\theta)$ .

MCTS was originally designed for discrete action environments, and is slightly less agnostic to continuous actions. We follow the popular approach of SampledMZ (Hubert et al., 2021), which showed that one can simply sample  $K$  actions from the prior policy at each node in the search tree, and treat  $\{a_1, \dots, a_K\}$  as a discrete action space, turning MCTS into a continuous-action-space algorithm.

Pseudocode for the different algorithms is provided below.

---

**Algorithm 1** Outer-Loop with Modular Search

---

**Require:** Search algorithm (planner)  $\mathcal{P}$ , neural networks  $\pi_{\theta_1}, V_{\phi_1}$ , replay buffer  $\mathcal{D}_{(1)} = \emptyset$ , environment's dynamics model  $\mathcal{M} = (P, R)$  and budget parameters  $B$ .

- 1: **for** episode  $n = 1$  to  $N$  **do**
- 2:     Sample starting state  $s_1 \sim \rho$ .
- 3:     **for** step  $t = 0$  to termination or timeout **do**
- 4:          $\pi_{improved}(s_t), V_{search}(s_t) \leftarrow \mathcal{P}(\pi_{\theta_n}, v_{\phi_n}, \mathcal{M}, B)(s_t)$ .
- 5:          $a_t \sim \pi_{improved}(s_t)$ .
- 6:          $s_{t+1} \sim P(\cdot | s_t, a_t), r_t \sim R(s_t, a_t)$ .
- 7:         Append  $(s_t, a_t, r_t, s_{t+1}, \pi_{improved}(s_t), V_{search}(s_t))$  to buffer  $\mathcal{D}_{(n)}$ .
- 8:     **end for**
- 9:     Update policy params  $\theta_{n+1}$  with SGD and CE loss on targets  $\pi_{improved}$  from  $\mathcal{D}_{(n)}$ .
- 10:    Update value params  $\phi_{n+1}$  with SGD and MSE loss on TD- $\lambda$  targets using  $V_{search}$  from  $\mathcal{D}_{(n)}$ .
- 11:    Set  $\mathcal{D}_{n+1} = \mathcal{D}_n$ .
- 12: **end for**

---



---

**Algorithm 2** RL-SMC

---

**Require:** Number of particles  $N$ , depth  $T$ , model  $P$ , prior-policy  $\pi_\theta$ , policy improvement operator  $I$ , value function  $Q^{\pi_\theta}$  and current state in the environment  $s_{root}$ .

- 1: Initialize particles  $n \in N$ , with  $w_0^n = 1$ ,  $s_1^n = s_{root}$ , and ancestor identifier  $\{j_1^n = n\}_{n=1}^N$  (which identifies per particle which action at the root it is associated with).
- 2: **for**  $t = 1$  to  $T$  **do**
- 3:     **Mutation:**  $\{a_t^n \sim \pi_\theta(a_t | s_t^n)\}_{n=1}^N, \{s_{t+1}^n \sim P(\cdot | s_t^n, a_t^n)\}_{n=1}^N$ .
- 4:     **Correction:**  $\{w_t^n = w_{t-1}^n \frac{\pi'(a_t^n | s_t^n)}{\pi_\theta(a_t^n | s_t^n)}, \pi'(s_t^n) = \mathcal{I}(Q^{\pi_\theta}, \pi_\theta)(s_t^n)\}_{n=1}^N$ .
- 5:     **Selection:**  $\{(j_t^n, a_t^n, s_{t+1}^n)\}_{n=1}^N \sim \text{Multinomial}(N, \text{normalized } w_t), \{w_t^n = 1\}_{n=1}^N$ .
- 6: **end for**
- 7: Return  $\{j_T^n, w_T^n\}_{n=1}^N$

---

---

**Algorithm 3** SMCTS

**Require:** Number of particles  $N$ , depth  $T$ , current state in the environment  $s_{root}$ , model  $\mathcal{M} = (P, R)$ , prior-policy  $\pi_\theta$ , value network  $v_\phi$ , improvement operators for search  $\mathcal{I}_{search}$  and root  $\mathcal{I}_{root}$ .

- 918 1: Initialize particles  $n \in N$ , with  $w_0^n = 1, s_1^n = s_{root}$  non-bootstrapped returns  $R_0^n = 0$ , and  
919 ancestor identifier  $\{j_1^n = n\}_{n=1}^N$ .
- 920 2: **for**  $t = 1$  to  $T$  across  $n$  particles in parallel **do**
- 921 3: *Mutation*:  $a_t^n \sim \pi_\theta(s_t^n)$ ,  $r_t^n \sim R(s_t^n, a_t^n)$ ,  $s_{t+1}^n \sim P(s_{t+1}^n | s_t^n, a_t^n)$ .
- 922 4: If  $t = 1$ , maintain the set of  $N$  root actions:  $A_1 \leftarrow \{a_1^n\}_{n=1}^N$ .
- 923 5: Approximate state-action value:  $Q(s_t^n, a_t^n) \leftarrow r_t^n + \gamma v_\phi(s_{t+1}^n)$ .
- 924 6: Compute the search policy:  $\pi'(s_t^n) \leftarrow \mathcal{I}_{search}(\pi_\theta, Q)(s_t^n)$ .
- 925 7: *Correction*: Compute importance sampling weights (Equation 11):  $w_t^n = w_{t-1}^n \frac{\pi'(s_t^n)}{\pi_\theta(s_t^n)}$ .
- 926 8: Update the non-bootstrapped returns:  $R_t^n = R_{t-1}^n + \gamma^t r_t^n$ .
- 927 9: Normalize importance sampling weights *per action at the root* using their identifiers  $j_t^n$ :

$$y_t^n = \frac{w_t^n}{\sum_{k=1}^N w_t^k \mathbb{1}_{j_t^n = j_t^k}}.$$

- 928 10: Estimate  $Q_t(s_{root}, \cdot)$  for initial actions  $a_1^n \in A_1$  using  $R_t^n$  and  $v_\phi(s_{t+1})$ :

$$Q_t(s_{root}, a_1^n) = \sum_i^N y_t^i (R_t^i + \gamma^{t+1} v_\phi(s_{t+1}^i)) \mathbb{1}_{j_1^n = j_t^i}$$

- 929 11: Update the running average  $\bar{Q}_t(s_{root}, \cdot)$  where  $Q_t(s_{root}, \cdot)$  is defined:

$$\bar{Q}_t(s_{root}, a_1^n) = \frac{(1-t)\bar{Q}_{t-1}(s_{root}, a_1^n) + Q_t(s_{root}, a_1^n)}{t}$$

- 930 12: *Selection*: Resample particles proportional to  $w_t$ , and reset  $w_t \leftarrow 1$ , as in Algorithm 2.

931 13: **end for**

- 932 14: Compute improved policy  $\pi_{improved}(s_{root}) \leftarrow \mathcal{I}_{root}(\pi_\theta, \bar{Q}_T)(s_{root})$ .

- 933 15: Compute the value of the improved policy across the set of root actions  $A_1$ :

$$V_{search}(s_{root}) \leftarrow \sum_{a_1^n \in A_1} Q_T(s_{root}, a_1^n) \pi_{improved}(a_1^n | s_{root}).$$

- 934 16: **Return**  $\pi_{improved}(s_{root}), V_{search}(s_{root})$ .

---

955  
956  
957  
958  
959  
960  
961  
962  
963  
964  
965  
966  
967  
968  
969  
970  
971

---

972 **Algorithm 4** TSMCTS

973 **Require:** Number of particles  $N$ , planning depth  $T$ , current state in the environment  $s_{root}$ , number  
 974 of actions to search at the root  $m_1$ , model  $\mathcal{M} = (P, R)$ , policy network  $\pi_\theta$ , value network  $v_\phi$ ,  
 975 Gumbel noise vector  $g$ .  
 976

1: Compute the per-iteration depth (Equation 17):  $T_{SH} \leftarrow T / \log_2 m_1$ .  
 977

2: Get  $m_1$  starting actions (Equation 18, left):  $A_1 = \{a_1, \dots, a_{m_1}\} \leftarrow \arg \max(\pi_\theta(s_{root}) + g, m_1)$ .  
 978

3: Initialize running sum of particles per action  $N^0(a) \leftarrow 0$  and running value sum per action  
 979  $Q_{sum}^0(s_{root}, a) \leftarrow 0$ , for all actions at the root  $a \in A_1$ .  
 980

4: Compute starting number of particles per action:  $N_1 \leftarrow \text{floor}(N/m_1)$ .  
 981

5: **for**  $i = 1$  to  $\log_2 m_1$  **do**  
 982

6:   **for** each action  $a \in A_i$  in parallel **do**  
 983

7:     Sample  $s_1 \sim P(\cdot | s_{root}, a)$ ,  $r_1 \sim R(s_{root}, a)$ .  
 984

8:     Search using SMCTS:  
 985

986        $V_{SMCTS}^i(s_1) \leftarrow \text{SMCTS}(N_i, T_{sh}, s_1, \mathcal{M}, \pi_\theta, v_\phi, \mathcal{I}_{GMZ}, \mathcal{I}_{GMZ})$ .  
 987

988 9:     Approximate the value of action  $a$ :  
 989

990        $Q_{SMCTS}^i(s_{root}, a) = r + \gamma V_{SMCTS}^i(s_1)$ .  
 991

992 10:   Update the running sums of particles and values of  $a$  (Equation 20):  
 993

994        $N^i(a) \leftarrow N^{i-1}(a) + N_i$ ,  $Q_{sum}^i(s_{root}, a) \leftarrow Q_{sum}^{i-1}(s_{root}, a) + N_i Q_{SMCTS}^i(s_{root}, a)$ .  
 995

996 11:   **end for**  
 997

998 12:   Compute the current iteration's value estimate at the root (Equation 19):  
 999

1000        $\forall a \in A_i : Q_{SH}^i(s_{root}, a) \leftarrow \frac{1}{\sum_{j=1}^i N(j, a)} \sum_{j=1}^i N(j, a) Q_{SMCTS}^j(s_{root}, a) = \frac{Q_{sum}^i(s_{root}, a)}{N^i(a)}$ .  
 1001

1002 13:   Update the number of actions to search:  $m_{i+1} = m_i/2$ .  
 1003

1004 14:   Update the actions to search (Equation 18, right):  $A_{i+1} \leftarrow \arg \max(Q_{SH}^i(s_{root}, \cdot), m_{i+1})$   
 1005

1006 15:   Update the running number of particles per action:  $N_{i+1} \leftarrow 2N_i$ .  
 1007

1008 16:   **end for**  
 1009

1010 17:   Compute the final Q-estimate (Equation 19):  
 1011

1012        $\forall a \in A_1 : Q_{SH}(s_{root}, a) \leftarrow \frac{Q_{sum}^{\log_2 m_1}(s_{root}, a)}{N^{\log_2 m_1}(a)}$ .  
 1013

1014 18:   Compute the improved policy  $\pi_{improved}$  using  $\mathcal{I}_{GMZ}$ :  
 1015

1016        $\forall a \in A_1 : \pi_{improved}(a | s_{root}) \leftarrow \frac{\exp(\beta Q_{sh}(s_{root}, a) + \log \pi_\theta(a | s_{root}) + g(a))}{\sum_{b \in A_1} \exp(\beta Q_{sh}(s_{root}, b) + \log \pi_\theta(b | s_{root}) + g(b))}$   
 1017

1018        $\forall a \notin A_1 : \pi_{improved}(a | s_{root}) \leftarrow 0$   
 1019

1020 19: And its value:  $V_{search}(s_{root}) = \sum_{a \in M_1} \pi_{improved}(a | s_{root}) Q_{sh}(s_{root}, a)$ .  
 1021

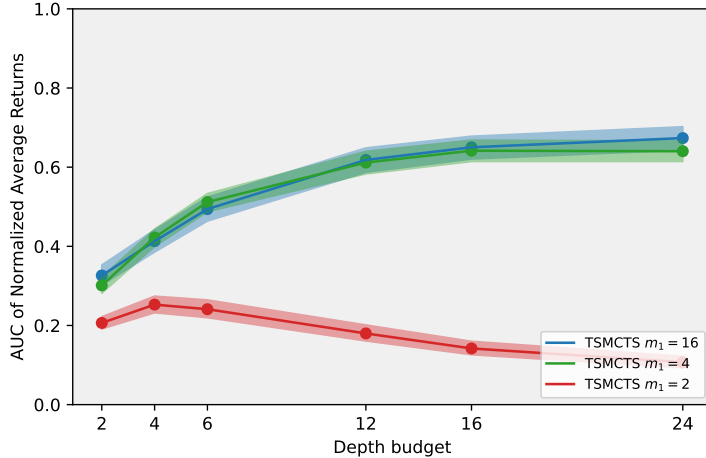
1022 20: Return  $\pi_{improved}(s_{root})$ ,  $V_{search}(s_{root})$ .  
 1023

1024

1025

---

1026 **C ADDITIONAL EXPERIMENTS**

1028 **Investigating the effect of the  $m_1$  parameter** We investigate the effect of the  $m_1$  parameter, the  
1029 number of actions that are searched at the root of TSMCTS in Figure 5. Performance is summarized as  
1030 area-under-the-curve (AUC) for the evaluation returns during training normalized across environments  
1031 with respect to minimum and maximum AUCs observed across agents and seeds. Clearly, limiting  
1032 the search to only the top two actions is strongly detrimental. On the other hand the confidence  
1033 bounds for  $m_1 = 4, 16$  almost entirely overlap, which suggest that for a sufficiently large  $m_1$  the  
1034 effect across environments is modest.

1051 Figure 5: Performance scaling with depth (higher is better, increasing is better). Averaged across  
1052 environments and particle budgets of 4, 8, 16 and normalized across environments. Mean and 90%  
1053 two-sided BCa-bootstrapped intervals across 10 seeds.

1055 **D EXPERIMENTS DETAILS**

1057 For the experiments, we build on the setup proposed by de Vries et al. (2025), which we describe in  
1058 more detail below.

1060 **Environments** We have used Jumanji’s (Bonnet et al., 2024) Snake-v1 and Rubikscube-partly-  
1061 scrambled-v0, as well as Brax’s (Freeman et al., 2021) Ant, Halfcheetah and Humanoid.

1063 **Compute** All experiments were run on the [anonymized for review] cluster with a mix of  
1064 [anonymized for review] GPU cards. Each individual run (seed) used 2 CPU cores and  $\leq 6$  GB of  
1065 VRAM.

1067 **Wall-clock Training Time Estimation** To estimate the training runtime in seconds (Figure 3), we  
1068 used an estimator of the the runtime-per-step (total runtime divided by steps) and multiplied this  
1069 by the current training step to obtain a cumulative estimate. This estimator should more robustly  
1070 deal with the variations in hardware, the compute clusters’ background load and XLA dependent  
1071 compilation. Of course, estimating runtime is strongly limited to hardware and implementation and  
1072 the results presented in Figure 3 should only be taken with that in mind.

1073 **Variance and Path Degeneracy Estimation** In Figure 4 center we plot the variance of the root  
1074 estimator  $V(s_0) = \sum_{a \in M} \pi_{improved}(a|s) Q_{search}(s, a)$  at the end of training as a function of depth  
1075 for each method.  $M$  is the number of actions over which the estimator maintains information  
1076 (susceptible to path degeneracy).

1078 Following de Vries et al. (2025), for TRT-SMC and the SMC baseline we compute  $Q_{search}$  as  
1079 the TD- $\lambda$  estimator for each particle at the root for the *last* depth  $t = T$ . If multiple particles are  
associated with the same action at the root, the particle estimates are averaged. To address path

1080 degeneracy when all particles for a root action are dropped TRT-SMC saves the last TD- $\lambda$  estimate  
 1081 for each root action. For T/SMCTS we use  $V_{T/SMCTS}$  respectively. In Figure 4 right we plot the  
 1082 number of actions at the root with which information is associated at the end of training,  $M$ , vs.  
 1083 depth.

1084

1085 **Neural Network Architectures** As specified by de Vries et al. (2025), which are themselves  
 1086 adapted from Bonnet et al. (2024) and Macfarlane et al. (2024) (e.g. MLPs in all environments except  
 1087 Snake where a CNN followed by an MLP is used).

1088

1089 **Hyperparameters** We've used the hyperparameters used by Macfarlane et al. (2024) and de Vries  
 1090 et al. (2025) for these tasks (when conflicting, we've used the parameters used by the more recent  
 1091 work (de Vries et al., 2025)). Except for the two new hyperparameters introduced by T/SMCTS no  
 1092 hyperparameter optimization took place. These new hyperparameters are (i)  $m_1$ , for which results are  
 1093 presented in Figure 5. (ii) The  $\beta_{root}$  inverse-temperature hyperparameter of  $\mathcal{I}_{GMZ}$  used by T/SMCTS  
 1094 to compute the improved policy at the root ( $\mathcal{I}_{root}$ ). For  $\beta_{root}$  we conducted a grid search with a small  
 1095 number of seeds across environments and values of  $0.1^{-1}, 0.05^{-1}, 0.01^{-1}, 0.005^{-1}$ .  $\beta = 0.01^{-1}$   
 1096 was overall the best performer. The  $\beta_{search}$  hyperparameter is actually the same parameter as the  
 1097 *target temperature* used by the SMC baseline (see de Vries et al., 2025). We have not observed  
 1098 differences in performance across a range of parameters  $\beta_{search}$  for TSMCTS and opted to use the  
 1099 same value as SMC.

1100

Hyperparameters are summarized in Tables 1, 2, 3, 4, 5 and 6.

Name	Value Jumanji	Value Brax
SGD Minibatch size	256	256
SGD update steps	100	64
Unroll length (nr. steps in environment)	64	64
Batch-Size (nr. parallel environments)	128	64
(outer-loop) Discount	0.997	0.99
Entropy Loss Scale ( $c_{ent}$ )	0.1	0.0003

Table 1: Shared experiment hyperparameters.

Name	Value Jumanji	Value Brax
Policy-Ratio clipping	0.3	0.3
Value Loss Scale	1.0	0.5
Policy Loss Scale	1.0	1.0
Entropy Loss Scale	0.1	0.0003

Table 2: PPO hyperparameters.

Name	Value Jumanji	Value Brax
Replay Buffer max-age	64	64
Nr. bootstrap atoms	30	30
Max depth	16	16
Max breadth	16	16

Table 3: GumbelMCTS hyperparameters.

Name	Value Jumanji	Value Brax
Replay Buffer max-age	64	64
Selection (Resampling) period	4	4
Target temperature	0.1	0.1
Nr. bootstrap atoms	30	30

Table 4: Shared SMC hyperparameters.

Name	Value Jumanji	Value Brax
(inner-loop) Retrace $\lambda$	0.95	0.9
(inner-loop) Discount	0.997	0.99
(outer-loop) Value mixing	0.5	0.5
Estimation $\pi_{improved}$	Message-Passing	Message-Passing

Table 5: TRT-SMC variance ablation hyperparameters.

Name	Value
Root policy improvement operator ( $\mathcal{I}_{root}$ )	$\mathcal{I}_{GMZ}$
Search policy improvement ( $\mathcal{I}_{search}$ )	$\mathcal{I}_{GMZ}$
Root inverse temperature $\beta_{root}$	$0.01^{-1}$
Search inverse temperature $\beta_{search}$	$0.1^{-1}$
Number of actions to search at the root $m_1$	4 (Figures 1,2,3), 16 (Figure 4)

Table 6: SMCTS and TSMCTS hyperparameters.